



# Soil processes govern alkalinity and cation retention in enhanced weathering for carbon dioxide removal

Jens S. Hammes<sup>1</sup>, Jens Hartmann<sup>2</sup>, Johannes A. C. Barth<sup>3</sup>, Tobias Linke<sup>2</sup>, Ingrid Smet<sup>1</sup>, Mathilde Hagens<sup>4</sup>, Philip A.E. Pogge von Strandmann<sup>5</sup>, Tom Reershemius<sup>6</sup>, Bruno Casimiro<sup>6</sup>, Arthur Vienne<sup>7</sup>,

5 Anna A. Stoeckel<sup>1</sup>, Ralf Steffens<sup>1</sup>, Dirk Paessler<sup>1</sup>

- <sup>1</sup> Carbon Drawdown Initiative, Fürth, 90766, Germany.
- <sup>2</sup> Department of Earth System Sciences, Universität Hamburg, Hamburg, 20146, Germany.
- <sup>3</sup> Department of Geography and Geosciences, GeoZentrum Nordbayern, Friedrich-Alexander- Universität Erlangen-Nürnberg (FAU), Erlangen, 91054, Germany.
- 0 <sup>4</sup> Soil Chemistry Group, Wageningen University & Research, Wageningen, 6700, Netherlands.
  - <sup>5</sup> MIGHTY (Mainz Isotope and Geochemistry Centre), Institute of Earth Sciences, Johannes Gutenberg University, Mainz, 55099, Germany.
  - <sup>6</sup> School of Natural and Environmental Sciences, Newcastle University, Newcastle-upon-Tyne, NE1 7RU, UK.
- Biobased Sustainability Engineering (SUSTAIN), Department of Bioscience Engineering, University of Antwerp, Antwerp,
   2020, Belgium.

Correspondence to: Jens S. Hammes (jens.hammes@carbon-drawdown.de)

Abstract. Avoiding the most damaging consequences of climate change will almost certainly require pairing rapid emission cuts with large-scale carbon dioxide removal (CDR). Among the proposed CDR pathways, enhanced weathering (EW) accelerates natural mineral dissolution to convert atmospheric CO2 into long-lived bicarbonate and carbonate reservoirs. Despite the many reported data from EW experiments, large uncertainty remains about the realisable CDR potential of applying rock materials to agricultural land. One of the relevant sinks for CO2 is the transfer to bicarbonate alkalinity, and various EW studies have reported a wide range of results for this process. Intercomparison of these data is problematic due to the different experimental set-ups, environmental conditions as well as combinations of rock materials and soil types. In order to assess and compare the realisable CDR potential of various EW combinations, a large greenhouse experiment was set up in which 4 different soil types (7 different soil batches) were treated with 13 different feedstock materials. The experiment included growing perennial ryegrass (Lolium perenne) and was conducted over two years with high irrigation rates (> 2000 mm a-1) and elevated temperatures (>19 °C) to speed up the weathering process. Alkalinity production was highly variable among the treatments and some even showed a loss of alkalinity compared to their controls. Consistent with expected dissolution kinetics, alkalinity production rates followed the trend: steel slag > limestone / carbonate-rich metabasalt > peridotite > basanite. Matrix analyses of soil properties versus feedstock revealed that alkalinity production from acidic soils was highest. At higher pHlevels (> 7 pH), carbonate mineral saturation likely constrains further dissolution, potentially favouring carbonate formation. Detailed analyses of cation pools (exchangeable, carbonates, oxides and clay) revealed large changes within the first year where 10-50 times more cations were retained than exported via leachate, making the realised CDR potential as alkalinity relatively small compared to the CDR potential of cations retained. Understanding the dynamics of transfers between cation





pools and their potential saturation are important to develop models and enable projections. Data reported from EW studies so far are insufficient to enable calibration of models, specifically if projections in CDR-realisations should span decades.

#### 1 Introduction

In order to limit global warming below 2 °C, climate mitigation strategies must involve drastic reductions in emissions besides actively removing CO<sub>2</sub> from the atmosphere (IPCC, 2018). Achieving the Paris Agreement's goal of limiting global warming by 2050 will require the annual removal of 7–9 billion tonnes of CO<sub>2</sub> (Smith et al., 2024). As no single approach is suitable for every ecological or geophysical context, this will necessitate a diverse portfolio of carbon-dioxide-removal (CDR) methods (Fuss et al., 2018; Medicine et al., 2019).

45 Land-based CDR approaches include afforestation, application of biochar to agricultural soils and enhanced weathering (EW), as well as engineered technologies such as bioenergy with carbon capture and storage (BECCS) and direct air carbon capture and storage (DACCS). Further approaches include ocean-based strategies, such as ocean alkalinity enhancement that increases the ocean's capacity to absorb and store CO<sub>2</sub>.

50 Among terrestrial strategies, enhanced weathering is particularly appealing due to its scalability, its additional ability to improve soil and plant health and its potential for long-term carbon sequestration (Beerling et al., 2020). EW involves amending soils with crushed silicate rocks (or other alkaline feedstocks) to accelerate their chemical weathering reaction with CO<sub>2</sub>. In soil and rainwater, dissolved CO<sub>2</sub> forms carbonic acid (H<sub>2</sub>CO<sub>3</sub>), which can react with silicate minerals (Berner et al., 1983; Walker et al., 1981). A classic example of this process is the dissolution of wollastonite (CaSiO<sub>3</sub>) (R1) (Almaraz et al., 2022; Hartmann et al., 2013):

$$CaSiO_3 + 2H_2CO_3 + H_2O \rightarrow Ca^{2+} + 2HCO_3^- + H_4SiO_4$$
 (R1)

This reaction sequesters atmospheric CO<sub>2</sub> by converting it into bicarbonate (HCO<sub>3</sub><sup>-</sup>) with carbonic acid as an intermediate, while releasing calcium (Ca<sup>2+</sup>). Similar reactions release other cations (e.g. Na<sup>+</sup>, K<sup>+</sup> or Mg<sup>2+</sup>) that charge-balance alkalinity, which contributes to long-term carbon storage in soil solutions, groundwaters, rivers and the ocean (Wolf-Gladrow et al., 2007). Alkalinity that reaches the oceans has a residence time of 88-121 thousand years (Middelburg et al., 2020) ultimately leading to the precipitation of carbonates or remaining dissolved as (bi)carbonate (Berner, 2003; Hartmann et al., 2013).

Further, this terrestrial form of CO<sub>2</sub> sequestration does not lead to land-use conflicts as it can be combined with agriculture and may even improve soil and crop health (Buss et al., 2024; Haque et al., 2019). It is therefore considered more sustainable than plant biomass carbon, which is often quickly returned to the atmosphere through decomposition of organic material (Fuss et al., 2018; Smith, 2005).

https://doi.org/10.5194/egusphere-2025-5402 Preprint. Discussion started: 24 November 2025 © Author(s) 2025. CC BY 4.0 License.





The fate of the released cations and associated alkalinity (mainly carbonate alkalinity: HCO<sup>3-</sup> & CO<sub>3</sub><sup>2-</sup>) determines the efficiency and permanence of CO<sub>2</sub> sequestration by EW, together with long-term changes in soil organic carbon (SOC) storage and CO<sub>2</sub> degassing from soils. Ideally, one mole of alkalinity will form for each mole of charge-equivalent released base cations (e.g. Ca<sup>2+</sup>, Mg<sup>2+</sup>, Na<sup>+</sup> and K<sup>+</sup>). However, the fate of cations after mineral dissolution is uncertain. Within soil pore water, cations may also charge-balance non-carbonate anions such as NO<sub>3</sub><sup>-</sup>. Base cations may be lost from the soil pore water in exchange for other cations via plant uptake and temporary adsorption onto cation exchange sites (CEC) on soil or organic particles, or by incorporation into newly formed minerals such as secondary carbonates, clay minerals, (hydro)oxides, or organic-mineral complexes (Kanzaki et al., 2025; Pogge von Strandmann et al., 2025; Sparks, 2003; Steinwidder et al., 2025; Tisdale et al., 1985; Wimpenny, 2016).

Although field trials are still essential for evaluating real-world feasibility, monitoring and sampling leachate and gas fluxes can be challenging in such open systems (Clarkson et al., 2024). As an alternative, closed systems in a controlled environment enable improved understanding of crucial processes. While a greenhouse mesocosm approach should not entirely replace field trials for quantifying CDR potential, it is more cost and labor-effective to test high numbers of rock/soil combinations in controlled environmental conditions than in the field. Controlled experiments can also be used to investigate longer-term processes, because weathering reactions are more rapid at constantly higher temperatures and water supply (West et al., 2005). Depending on the design of experiments, an initial 'flushing period' of cations is often observed within the first few weeks of setting up soil column or pot experiments (Amann et al., 2022; Vorrath et al., 2025). This phenomenon can influence early measurements of cation release, CO<sub>2</sub> efflux and alkalinity generation and has been observed in previous studies (e.g. Amann et al., 2020). This has been attributed to the 'Birch effect' that in this case happens because of disturbance (sieving, drying and rewetting) of the soil system during experiment preparation and setup (Birch, 1958; Smith et al., 2023). Such disturbances can lead to preferential release of soluble ions, increasing mineralisation of organic matter and CO<sub>2</sub> efflux, desorption from cation exchange sites or displacement of pore water. These mechanisms may affect the interpretation of short-term experiments when used to interpolate for long-term weathering processes. Therefore, interpretation of long-term CO<sub>2</sub> sequestration requires understanding of initial adjustment phases and their rate changes of cation release.

Most published research on pot, column or mesocosm trials investigating the potential of enhanced weathering (EW) to sequester CO<sub>2</sub> and the fate of released cations relies primarily on short-term experiments that typically last from a few weeks to a few months. Examples of known test periods are 8 weeks (Haque et al., 2019); 64 days (te Pas et al., 2025); 99 days (Vienne et al., 2022); 120 days (Kelland et al., 2020); 5 months (Renforth et al., 2015); 6 months (Pogge von Strandmann et al., 2022b); 32 weeks (Ten Berge et al., 2012); 340 days (Amann et al., 2020). To the best of our knowledge, the only long-term pot trial monitoring leachate alkalinity with multiple feedstocks is by Buckingham & Henderson (2024), lasting 16 months, with collection of soil solutions in 13 sampling events. By combining a longer experimental phase under controlled

https://doi.org/10.5194/egusphere-2025-5402 Preprint. Discussion started: 24 November 2025

© Author(s) 2025. CC BY 4.0 License.





00 conditions, with multiple soils and feedstocks and high-frequency sampling, we were able to separate short-term dynamics from longer-term shifts.

Here, we present a comprehensive dataset from an approximately two year long greenhouse mesocosm trial of EW with cultivation of Lolium perenne (perennial ryegrass) in 10-litre buckets. The diverse set of experiments was designed to investigate the export of alkalinity in leachate waters Initial experiments began in January 2023 with four replicates for each treatment. A second group of experiments started in January 2024 and included seven replicates for each soil-feedstock combination.

Over the last two years, we have conducted around 400 pot tests, and all of this data is available on Github. Although our trials included various soil types and feedstocks that might be suitable for EW, this work focuses on a select number of setups where a specific feedstock was applied to several different soils, or where a diverse range of feedstocks was applied to one specific soil (197 pot trials). The materials investigated represent a variety of commonly studied EW amendments (e.g. peridotite, basanite (low-Si basalt), metabasalt, glacial rock flour, limestone, cement and steel slag), tested on numerous soils of European temperate climate (Hartmann et al., 2024). These experiments were conducted in a greenhouse with elevated temperatures (>19 °C all year) and high irrigation rates (2000 to 4000 mm a<sup>-1</sup>). It is therefore important to note that this study provides results under accelerated weathering conditions rather than real-field conditions in a temperate climate.

The leachate data presented here cover either 250 or 650 days of observation, from a total of 197 experimental setups, depending on the start date. This data set is unprecedented in terms of its long experimental duration and coverage of a variety of EW amendments applied to numerous soils of European temperate climate. It is providing a valuable opportunity to evaluate the potential of EW through alkalinity production in different agricultural soils. In addition to monitoring the leachate alkalinity, potential alkalinity sinks within the soil were investigated in a subset of experiments by measuring carbonate formation, cations trapped on exchange sites, and cations in other secondary phases. Our hypothesis is that alkalinity export from soils is higher following the application of alkaline materials for the purpose of EW. Our results provide valuable insights for cation and carbon accounting in EW deployments, including the role of soil cation sinks.

## 2 Experimental set up and analytical methods

## 2.1 General experimental design

Given the objectives of this study and the need for controlled comparisons between different soil types and their treatments, a controlled greenhouse mesocosm experiment was selected as the most appropriate approach. This design allows for detailed investigation under uniform conditions and ensures that observed differences in weathering rates and chemical transformations are primarily driven by soil characteristics and rock amendments, rather than by external environmental variability.

https://doi.org/10.5194/egusphere-2025-5402 Preprint. Discussion started: 24 November 2025 © Author(s) 2025. CC BY 4.0 License.





Each mesocosm comprised a stacked pair of 10-litre lysimeters (average Ø ≈ 25.6 cm, height 26.3 cm) that formed a closed soil-water-gas system (Fig. 1). The bottom bucket functioned as a leachate collection tank. Two push-in fittings, one near the base and one near the rim, were linked by a transparent PVC tube which was used to measure the leachate level as well as to drain during sampling. The upper port also allowed for headspace gas sampling. This tank was sealed to the upper 'soil' bucket by a perforated lid with silicone sealant around the edge. The base of this upper bucket was lined with root fleece and a 3 cm layer of washed quartz sand to ensure an even flow and to prefilter the leachate (Fig. 1). Above the sand, 10 cm of unamended soil was topped by ~15 cm of the treatment mix (sieved soil plus EW feedstock, see Tab. 1). In selected pots, electronic CO₂ sensors (NDIR-CO₂ Sensor 'Sensirion SCD30 CO₂') were embedded in the upper soil-rock horizon to measure pCO₂. To monitor how the feedstock surface area, mass and mineralogy might change over time, a tea-bag test sachet filled with 5 g of feedstock was added in the top layer of selected experiments. Note that these tea bag samples are not further discussed in this work, but are mentioned here as they may have also added weathering products to the leachate. Finally, 20 earthworms (mix of Eisenia foetida, Dendrobena veneta, Lumbricus terrestris) were added to each pot to allow bioturbation and 3 g of Lolium perenne seeds were uniformly distributed on top.

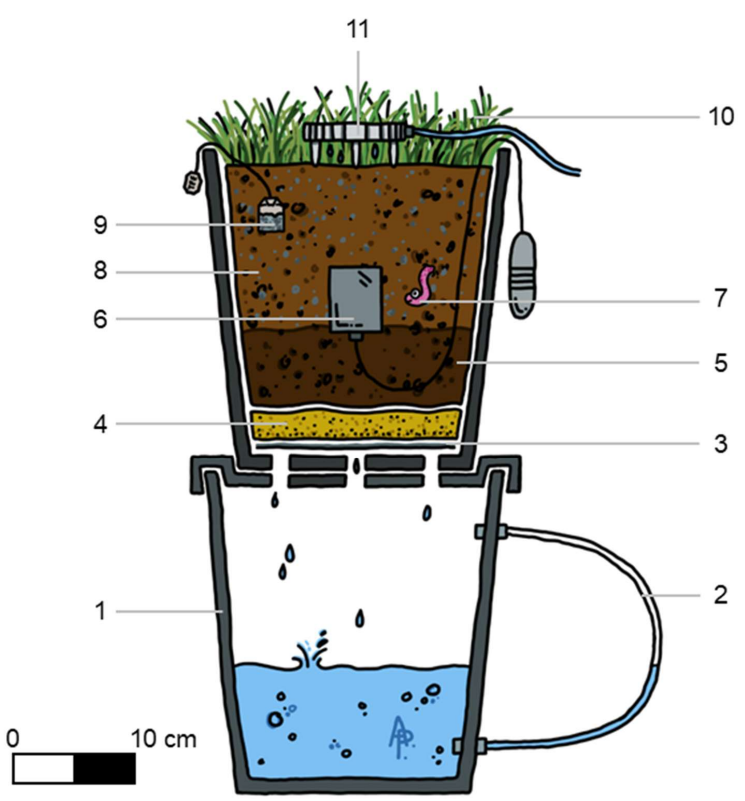
145 This greenhouse setting ensured that all mesocosm experiments experienced identical climatic conditions, thus allowing for accelerated weathering conditions. Moreover, having a temperature constantly above 19 °C (temperature range Fig. S1) and high leachate formation due to irrigation up to 2,000 mm a<sup>-1</sup> allowed for a shorter experimental period necessary to detect different biogeochemical trends.

To maintain a broadly consistent chemical composition and low background alkalinity, irrigation water was supplied from a rainwater cistern. The irrigation system (Netafim's Netbow irrigation rings with 4 outlets and a diameter of 12 cm) was automated to deliver water four times a day in six-hourly intervals to ensure consistent and comparable levels of soil moisture. During the hot summer months, the irrigation rate needed to be increased up to 4,000 mm a<sup>-1</sup> to ensure leachate formation due to the very high evapotranspiration rates (Tab. S5. Irrigation rates applied by period).

In addition, the mesocosm design allowed precise control of experimental variables such as rock amendment application and easy access for leachate sampling. Our experimental design also simplified logistical demands to accommodate large-scale monitoring across a total of 400 mesocosms in one site.







1 Leachate tank; 2 Transparent PVC tube; 3 Root fleece; 4 Filter sand; 5 Pure soil layer;
6 CO<sub>2</sub> Sensor; 7 Earthworm; 8 Layer of soil-feedstock mix; 9 Tea bag; 10 Lolium Perenne;
11 Irrigation ring.

Figure 1: Schematic sketch of Carbdown greenhouse mesocosm. Modified after Paessler et al. (2023).

160





 $Table\ 1.\ Overview\ of\ soils, treatments, replication\ across\ experimental\ batches\ and\ starting\ dates.$ 

LUFA 2.1	LUFA 2.2 A	LUFA 2.2 B	LUFA 6S A	LUFA 6S B	Fürth 2	
Started 01/2023	Started 01/2023	Started 01/2024	Started 01/2023	Started 01/2024	Started 04/2023	Started 05/2023
Controls n=4 Basanite 40 t ha-1 n=4 Metabasalt 40 t ha-1	Controls n=4 Basanite 40 t ha-1 n=4 Metabasalt 40 t ha-1	Controls n=7  Basanite 40 t ha-1 n=7  Limestone 10 t ha-1	Controls n=4 Basanite 40 t ha-1 n=4 Metabasalt 40 t ha-1	Controls n=7 Basanite 40 t ha-1 n=7 Limestone 10 t ha-1	Controls n=4 Cement concrete EW 1 40 t ha-1 n=4 (meta) Leuco-basalt EW 2 40 t ha-1	Controls n=4  Basanite 40 t ha-1 n=4  Basanite 200 t ha-1
n=4 Peridotite 40 t ha-1 n=4 Steel slag 40 t ha-1 n=4	n=4 Peridotite 40 t ha-1 n=4 Steel slag 40 t ha-1 n=4	n=7 Peridotite 40 t ha-1 n=7 Steel slag 40 t ha-1 n=7	n=4 Peridotite 40 t ha-1 n=4 Steel slag 40 t ha-1 n=4	n=7 Peridotite 40 t ha-1 n=7 Steel slag 40 t ha-1 n=7	n=4 (meta) Leuco-basalt EW 3 40 tha-1 n=4 Serpentinised peridotite EW 4 40 t ha-1 n=4	n=3
		Glacial Rock Dust 40 t ha-1 n=4			Serpentinised peridotite EW 5 40 t ha-1 n=4 Serpentinite EW 6 40 t ha-1 n=4 Leuco-basalt EW 7 40 t ha-1	
	Started 01/2023 Controls n=4 Basanite 40 t ha-1 n=4 Metabasalt 40 t ha-1 n=4 Peridotite 40 t ha-1 n=4 Steel slag 40 t ha-1	Started         Started           01/2023         01/2023           Controls         Controls           n=4         n=4           Basanite         Basanite           40 t ha-1         40 t ha-1           n=4         Metabasalt           Motabasalt         40 t ha-1           n=4         n=4           Peridotite         Peridotite           40 t ha-1         n=4           Steel slag         Steel slag           40 t ha-1         40 t ha-1	Started         Started         Started           01/2023         01/2024           Controls         Controls           n=4         n=7           Basanite         Basanite           40 t ha-1         40 t ha-1           n=4         n=7           Metabasalt         Limestone           40 t ha-1         10 t ha-1           n=4         n=7           Peridotite         Peridotite           40 t ha-1         40 t ha-1           n=4         n=7           Steel slag         Steel slag           40 t ha-1         n=7           Steel slag         Steel slag           40 t ha-1         n=7           Glacial Rock           Dust 40 t ha-1	Started         Started         Started         O1/2023         O1/2023           Controls         Controls         Controls         Controls           n=4         n=4         n=7         n=4           Basanite         Basanite         Basanite           40 t ha-1         40 t ha-1         40 t ha-1         40 t ha-1           n=4         n=7         n=4           Metabasalt         Limestone         Metabasalt           40 t ha-1         10 t ha-1         40 t ha-1           n=4         n=7         n=4           Peridotite         Peridotite         Peridotite           40 t ha-1         40 t ha-1         40 t ha-1           n=4         n=7         n=4           Steel slag         Steel slag         Steel slag           40 t ha-1         40 t ha-1         40 t ha-1           n=4         n=7         n=4      Steel slag  40 t ha-1  n=4   Glacial Rock  Dust 40 t ha-1	Started         Started         Started         Started         Started         O1/2023         01/2024         O1/2023         O1/2024           Controls         Controls         Controls         Controls         Controls         Controls           n=4         n=4         n=7         n=4         n=7           Basanite         Basanite         Basanite         Basanite           40 t ha-1         40 t ha-1         40 t ha-1         40 t ha-1           n=4         n=7         n=4         n=7           Metabasalt         Limestone         Metabasalt         Limestone           40 t ha-1         40 t ha-1         40 t ha-1         10 t ha-1           n=4         n=7         n=4         n=7           Peridotite         Peridotite         Peridotite         Peridotite           40 t ha-1         40 t ha-1         40 t ha-1         40 t ha-1           n=4         n=7         n=4         n=7    Steel slag  Steel slag  40 t ha-1  n=4  n=4  n=7  Glacial Rock  Dust 40 t ha-1  n=4  Dust 40 t ha-1	Started   Started   Started   Started   Started   O1/2023   O1/2024   O1/2023   O1/2024   O4/2023   O1/2024   O4/2024   O4/2023   O1/2024   O4/2024   O4/2023   O1/2024   O4/2024   O4/2

# 2.2 Soils

The soils selected for this experiment are of diverse origins. Two soils were sourced from the Carbon Drawdown Initiative's field trial site in Fürth, Germany: 'Fürth 1' was sampled in January 2023 for comparison with earlier field and lysimeter experiments at this site. 'Fürth 2' was sampled from the same field in late March 2023 for use in further pot trials. Three standardised soils from the Speyer Agricultural Research Institute (LUFA) were also used: LUFA 2.1, LUFA 2.2 and LUFA





6S. (Note: LUFA is a government-run, independent agricultural testing and research institute in Germany that provides standardised soils for agricultural experiments.) As two experiment series were conducted using different batches of LUFA 2.2 and LUFA 6S, the first batches are listed as LUFA 2.2 A and LUFA 6S A, while the second batches are listed as LUFA 170 2.2 B and LUFA 6S B.

Particle-size distributions were determined by dry sieving with DIN-compliant meshes (approximate aperture sequence: 630 μm, 200 μm, 63 μm). For ease of comparison with the international literature, we report texture names using the United States Department of Agriculture (USDA) classification. Texture names derived from these fractions, acknowledging a minor mismatch between systems (DIN uses 63 μm for the sand–silt boundary, whereas USDA uses 50 μm; clay is <2 μm in both schemes). This choice allows readers to directly compare our grain-size distributions with published datasets that use USDA terminology. The corresponding German soil texture classes following the 'Bodenkundliche Kartieranleitung' (KA6) (Hartmann et al., 2024), calculated from the same sieve data, are provided in the supplementary (Tab. S1).

The Fürth soils are loamy sands, which represent the second highest pH (7.1) of our tested batch. They also have a moderate cation exchange capacity (Fürth 1: 10.7 and Fürth 2: 10.2 meq (100 g)<sup>-1</sup>), and contain both some organic (0.97-1.08 wt%) and inorganic (0.14-0.15 wt%) carbon. The clay sample LUFA 6S is characterised by a slightly higher pH (7.3) with a high CEC (18.7-19.09 meq (100 g)<sup>-1</sup>) and roughly double the amounts of organic (1.46-2.05 wt%) and inorganic (0.26-0.37 wt%) carbon. In comparison to these slightly alkaline soils, the other two LUFA soils have an acidic pH and negligible soil inorganic carbon. LUFA 2.2 is a sandy loam with pH 5.6, moderate CEC (8.5-9.46 meq (100 g)<sup>-1</sup>) and the overall highest organic carbon (1.94-1.97 wt%). Finally, the LUFA 2.1 soil is a sand with the lowest pH (4.6), low CEC (2.9 meq (100 g)<sup>-1</sup>) and intermediate organic carbon contents (1.28 wt%). Detailed characterisation of the different batches of these 4 main soil types can be found in Table S1 of the Appendix (includes method description for pH, CEC, PSD and carbon).

# 2.3 Feedstock materials

A total of 13 different feedstock materials were used in this study. All feedstocks were applied to the mesocosms at 40 t ha<sup>-1</sup> to except limestone, which was applied at 10 t ha<sup>-1</sup>. These feedstock included 6 representative materials: serpentinised peridotite (referred to subsequently as "peridotite"), basanitic leucitite ("basanite"), greenlandic glacial sediment ("glacial rock flour"), calcite-rich metabasalt ("metabasalt"), industrial by product "steel slag", and dolomitic limestone ("limestone"). Additionally, 7 feedstocks were sourced from EW suppliers. For the basanite only, different application rates of the same feedstock (20, 40, 100, 200, 400 t ha<sup>-1</sup>) were added to investigate the relationship with alkalinity export.

For this study, we focus on a subset of 6 representative feedstocks, which were added to multiple soils. A short description of these materials is given below (more details can be found in the appendix: mineralogy (Tab. S2), chemistry (Tab. S3) and grain size and specific surface area (Tab. S4)).





## 2.4 Leachate sampling and analyses

Leachate water samples were collected monthly. The first milliliters of water were used to rinse all sampling containers before 200 being discarded, and this volume was also accounted for in the total volume of leachate measured during each sampling event.

## 2.4.1 Total Alkalinity

Total alkalinity (TA) for each mesocosm was measured on 100 ml of leachate with a HACH Digital Titrator (Model 16900 (SD ± 1 %)). This kit uses an indicator powder (Bromocresol Green-Methyl Red), which shows a colour change from green to red at pH 4.3. For the titration, sulphuric acid (1.6 N) was added to the sample dropwise until the titration end point was reached. According to the HACH titrator instructions, this amount of added acid is expressed as mg/l CaCO<sub>3</sub>. To convert this reading to mg/l HCO<sub>3</sub><sup>-</sup>, we use a factor of 1.22, derived from the molar ratios of CaCO<sub>3</sub> and HCO<sub>3</sub><sup>-</sup>. The resulting HCO<sub>3</sub><sup>-</sup> concentration in mg/l is then divided by 61 (the molar mass of HCO<sub>3</sub><sup>-</sup>) to turn the reading into in micromoles (μmol(eq) l<sup>-1</sup>). Note that this result primarily represents HCO<sub>3</sub><sup>-</sup>, but it may also include other negatively charged species that buffer H<sup>+</sup>. Therefore, we present the charge equivalent as alkalinity rather than the bicarbonate concentration.

#### 2.4.2 In situ measurement of pH, conductivity, O<sub>2</sub> and temperature

To determine in situ parameters such as pH, electrical conductivity (EC) and oxygen saturation and concentration, 200 ml of leachate was filled into a pre-rinsed measuring cylinder and measured with a portable WTW multi-parameter analyser (MultiLine® Multi 3630 IDS) and its sensors Sentix® 940-x (pH sensor (SD ± 0.1 pH unit)), TertraCon® 925 (EC sensor (SD ± 5 μmS cm<sup>-1</sup>)), FDO® 925 (Optical IDS dissolved oxygen sensor (SD dissolved O<sub>2</sub> conc. 0.2 mg l<sup>-1</sup>, O<sub>2</sub> saturation ± 2 %)). In order to obtain the leachate temperature in parallel with the sampling event, we always recorded the average value of the three built-in temperature sensors.

## 2.4.3 Major cations

Sample preparation consisted of filtration using 0.45  $\mu$ m nylon syringe disc filters (Minisart HighFlow PES, Sartorius AG, Germany) to remove suspended particles prior to analysis. The samples were then collected in 15 ml polypropylene conical centrifuge tubes (VWR Ultra-High Performance, HDPE-Cap with sealing ring, VWR International GmbH, Darmstadt, Germany) and acidified with 2 ml of 65 % HNO<sub>3</sub> to prevent precipitation and to stabilise the sample. Immediately after filling the sample tubes, they were cooled to 4  $^{\circ}$ C.

The stabilised water samples for major cation (Na<sup>+</sup>, K<sup>+</sup>, Ca<sup>2+</sup>, Mg<sup>2+</sup>) measurements were analysed three times for accuracy using inductively coupled plasma mass spectrometry (ICP-MS) (iCAP Qc, Thermo Fisher Scientific Inc., Bremen, Germany) as described in Bandara et al. (2023). For major cation calibration, a mixed standard was prepared from four single-element stock solutions (VWR; 1,000 ppm each of Ca, Mg, Na and K). A three-point external calibration curve was generated by serial dilution, with concentrations ranging from 0.4 to 2 ppm for K, Na and Mg, and from 4 to 20 ppm for Ca.

https://doi.org/10.5194/egusphere-2025-5402 Preprint. Discussion started: 24 November 2025

© Author(s) 2025. CC BY 4.0 License.





## 2.4.4 Major anions

Samples were also filtered using 0.45 µm nylon syringe disc filters and collected in 15 ml polypropylene conical centrifuge tubes, but not acidified.

Anions (F<sup>-</sup>, Br<sup>-</sup>, Cl<sup>-</sup>, NO<sub>3</sub><sup>-</sup>, NO<sub>2</sub><sup>-</sup>, SO<sub>4</sub><sup>2-</sup> and PO<sub>4</sub><sup>3-</sup>) were quantified by ion chromatography (930 Compact IC Flex, Deutsche Metrohm GmbH & Co. KG, Filderstadt, Germany). The limit of quantification was 0.1 mg l<sup>-1</sup> with a precision of <5 % RSD, verified by repeated measurements of two control standards as unknowns in the upper and lower calibration range.

# 2.5 Soil sampling and analyses

235 Soil samples were collected at the end of each experiment (i.e. after 250 and 650 days), or when a replicate pot was removed from the trial (only possible for the LUFA 2.2 B and 6S B trial because of sufficient replicates (n = 7)). Intermediate soil sampling was not performed in order to avoid disturbing the hydrological properties of ongoing experiments, which could compromise the representativeness of subsequent leachate data.

Upon sampling, the soil column from each pot was divided into either two or three layers of equal thickness depending on the experimental design. Each soil layer was homogenised immediately after sampling. A subsample of at least 800 g wet weight was then separated and placed in an aluminium tray to dry in a convection oven at 40 °C. After drying, the samples were ground using a mortar to ensure complete homogenisation prior to further analysis.

#### 2.5.1 Major and trace element chemistry of different soil fractions

Soil major and trace metal concentrations were measured for four different soil chemical fractions/pools, using a sequential extraction scheme (modified from Tessier et al. (1979), Pogge von Strandmann et al. (2022a), and Vienne et al. (2025)). The extractions targeted 1) the exchangeable fraction; 2) the carbonate fraction; 3) the reducible (oxides) fraction and 4) the clay mineral (primary and secondary) fraction. All extractions were carried out sequentially using 1.00 g of air-dried, homogenised soil. The supernatant solution was collected in full for analysis after each extraction step. Table 2 shows the volume and concentration of each extractant solution used, and the protocol used for each step.

250





Table 2: Extractant solutions and protocol used for soil sequential extractions. After: Tessier et al. (1979), Pogge von Strandmann et al. (2022a), and Vienne et al. (2025).

Soil	Extractant Solution	Protocol
Fraction/Pool		
1. Exchangeable	1M ammonium acetate (10 ml)	Add reagent; shake (20 °C, 1 h); centrifuge (2000
		rpm, 10 min)
2. Carbonate	A) 1M acetic acid (5 ml)	Add reagent A; shake (20 °C, 2 h); add reagent B;
	B) deionised water (4 ml) + 3M ammonium	centrifuge (2000 rpm, 10 min)
	acetate (1 ml)	
3. Reducible	0.04M hydroxylamine hydrochloride in 25%	Add reagent; shake (20 °C, 1 h); centrifuge (2000
(Oxide)	(v/v) acetic acid (20 ml)	rpm, 10 min)
4. Clay	0.6M hydrochloric acid (10 ml)	Add reagent; water bath (85 °C, 1 h); centrifuge
		(2000 rpm, 10 min)

Samples for each extracted soil fraction were analysed using ICP-OES (Agilent 5800) for Al, Ba, Ca, Cu, Fe, K, Mg, Mn, Na, P, S, Si, Sr, and Zn; and ICP-MS (Agilent 8900 Triple-Quadrupole using He or no collision cell gas) for Li, Ti, V, Cr, Co, Ni, As, Zr, Cd, Pb, Th, and U. Calibration standards and blanks for ICP-OES and ICP-MS analyses were matrix-matched to the extractant solutions for each fraction.

The internal analytical uncertainty of ICP-OES and ICP-MS measurements was assessed using a calibration standard as a drift monitor and a reference standard solution (Evian water). For each batch, all sequential extraction and analysis steps were performed in triplicate on one soil sample, to assess total measurement uncertainty.

#### 3 Results

# ${\bf 3.1}\ Leach at e\ total\ alkalinity\ export\ from\ specific\ soils$

The long-term dataset provides a comprehensive view of the temporal evolution of leachate alkalinity across 197 examined pots. Monthly sampling intervals enabled a robust and detailed assessment of changes in alkalinity over time. Results were normalised to one square meter soil surface area to facilitate comparison with field data. Figure 2 shows that cumulative alkalinity export from the mesocosms is not always higher than the controls. Specifically, the Fürth 1 soil shows significantly lower alkalinity export rates for some treatments.





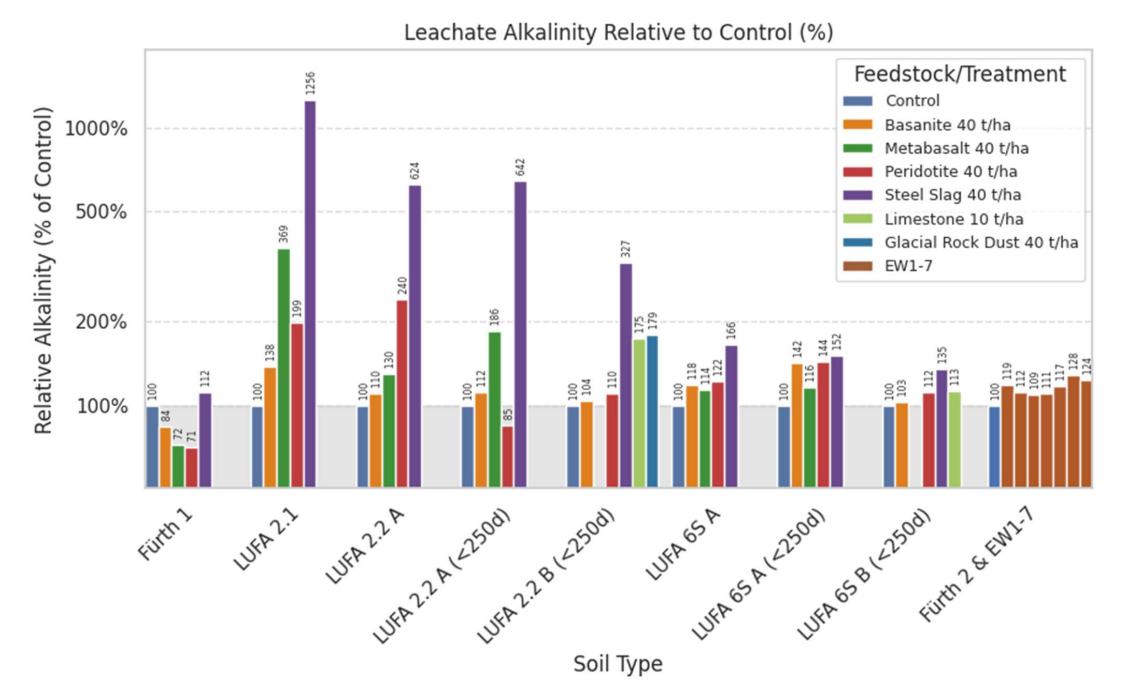


Figure 2: Relative cumulative leachate alkalinity between control pots and treated pots. Data from 650 days are available for Fürth 1, LUFA 2.1, LUFA 2.2 A and LUFA 6S A. To compare the two batches of LUFA soils built separately, the first 250 days of LUFA 2.2 A (started in 01.2023) and LUFA 6S A (started in 01.2023) are plotted separately next to the B batches (started in 01.2024). On Fürth 2 soil we tested 7 rock dusts from EW companies ('EW1-7'). Vertical numbers above columns indicate the exact percentages.

# 3.1.1 TA export from the loamy sand 'Fürth 1'

All treatments show a steady increase in accumulated alkalinity over the 650 day experiment. The control (blue) exports around ~7700 mmeq m<sup>-2</sup> alkalinity by the end of the experiment, in an almost linear pattern over time. Treatments with basanite (orange), metabasalt (green), and peridotite (red) followed a similar trend until day 200, after which export rates decreased, resulting in a lower cumulative TA production of 71 to 84 % relative to the control (Fig. 3). In contrast, the steel slag treatment (purple) showed a 12 % higher alkalinity export than the control.



280



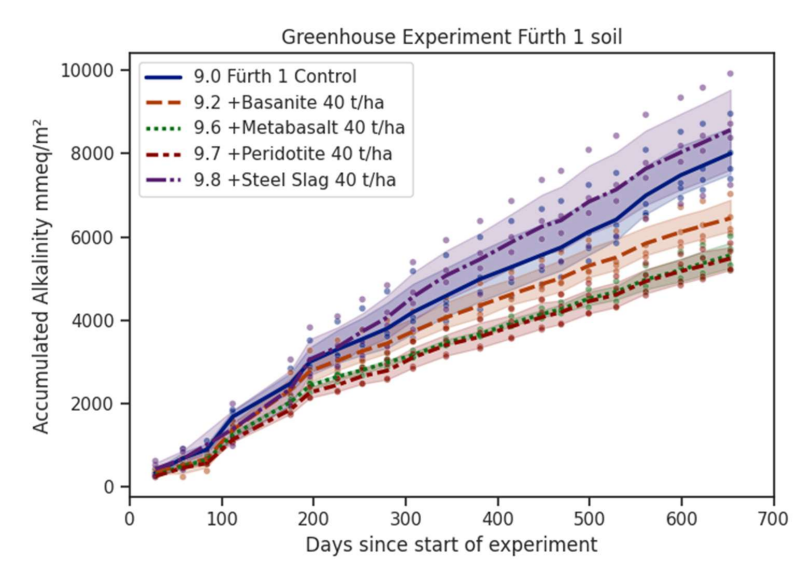


Figure 3: Accumulated leachate alkalinity results for Fürth 1 (n=4 per treatment). The control treatment (blue) consists only of the 'Fürth 1' soil, while the other experiments include additions of EW feedstock materials at 40 t ha-1 equivalent: basanite (orange), metabasalt (green), peridotite (red), and steel slag (purple). Shaded areas represent the variability among replicates.

## 3.1.2 TA export from the sand soil "LUFA 2.1"

285 The sandy LUFA 2.1 control released about one-ninth the alkalinity of the Fürth 1 control. In LUFA 2.1, all feedstock treatments increased the export rates. However, these rates remained below those of the Fürth 1 soil, except for the steel slag treatment (Fig. 4). Note that analyses of leachate samples started after an initial 140 day period. This delay was intentional, because high turbidity of early leachates interfered with accurate titration.

Measurements from the steel slag treatment started a month later because insufficient leachate was available until day 145.

13



290



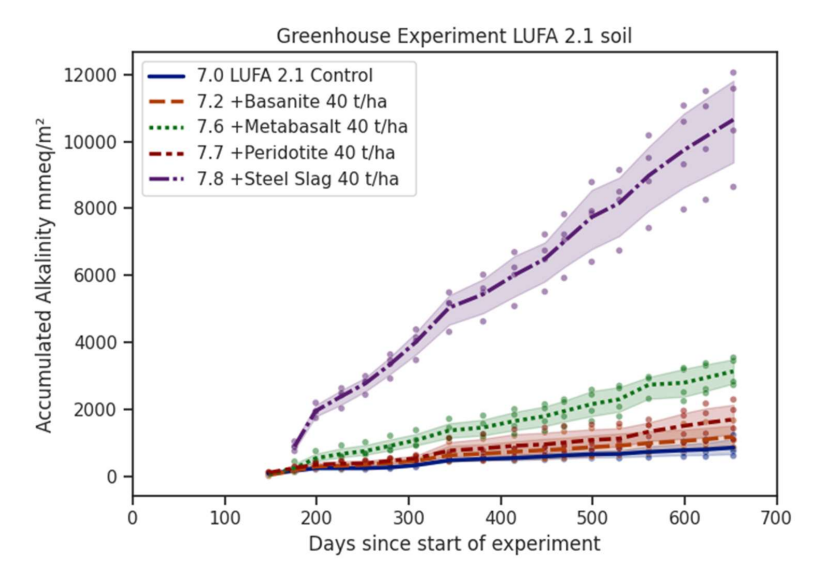


Figure 4: Accumulated leachate alkalinity results for LUFA 2.1 (n=4 per treatment). The control treatment (blue) consists only of the 'LUFA 2.1' soil, while the other experiments included additions of EW feedstock materials at 40 t ha<sup>-1</sup> equivalent: basanite (orange), metabasalt (green), peridotite (red), and steel slag (purple).

## 3.1.3 TA export from the sandy loam "LUFA 2.2"

The sandy loam LUFA 2.2 shows higher export rates than LUFA 2.1, but lower than Fürth soil, with the exception of the steel slag treatment with 11,800 mmeq m<sup>-2</sup> (Fig. 5a). The basanite and peridotite show, however, no clear deviation from the control, in contrast to the carbonate-rich metabasalt. The second experiment with LUFA 2.2, which ran for a shorter time period, reveals a similar pattern, but reaches much higher total accumulated alkalinity. These LUFA 2.2 B experiments again show no clear difference between control, basanite and peridotite. Two additional treatments, limestone at a 4x lower dose and glacial rock flour from Greenland (Fig. 5b), showed a significant increase in alkalinity export, resulting in accumulated TA values about twice as high as the control, and over half that of the steel slag.

14





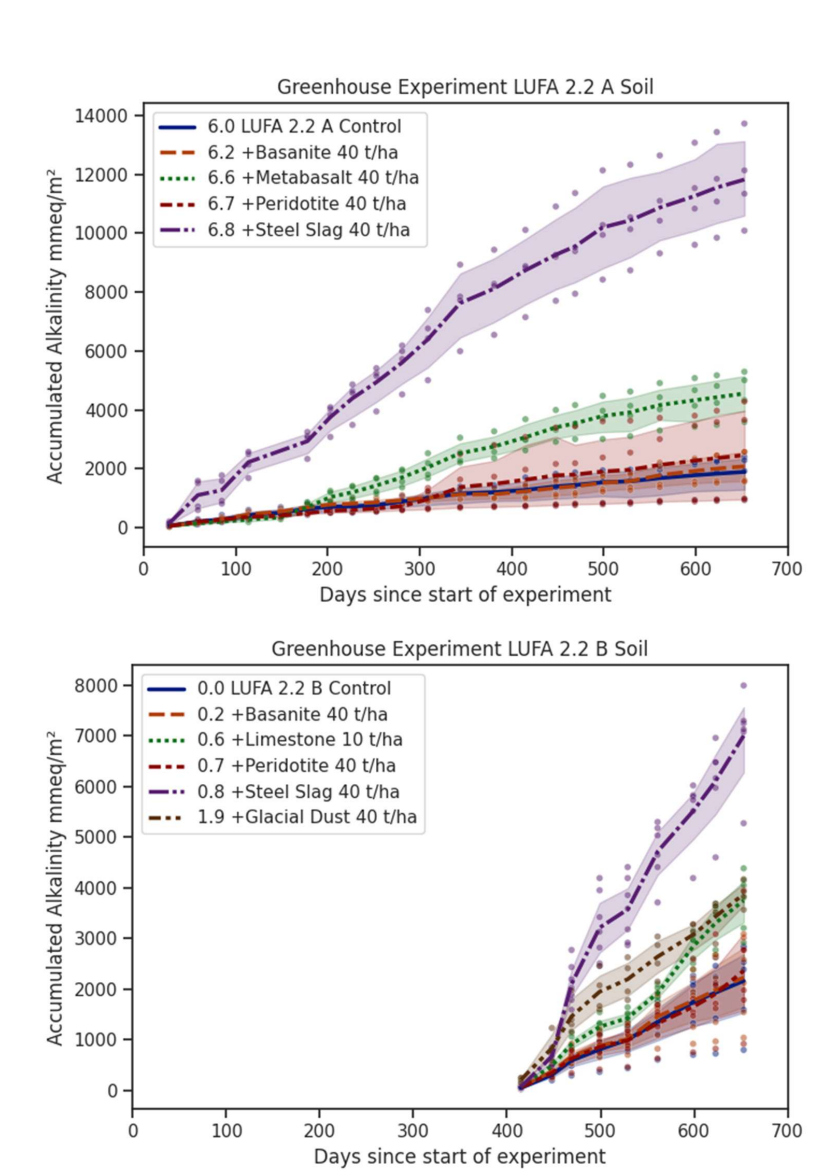


Figure 5: Accumulated leachate alkalinity results for LUFA 2.2. 5a: The control treatment (blue) consisted only of the first batch A of 'LUFA 2.2' soil, while the other experiments included additions of EW feedstock materials at 40 t ha<sup>-1</sup> equivalent: basanite (orange), metabasalt (green), peridotite (red), and steel slag (purple) (n = 4 per treatment). 5b: The control treatment (blue) consisted only of the second batch B of 'LUFA 2.2' soil, while the other experiments included additions of EW feedstock materials at 10 t/ha equivalent: limestone (green) or at 40 t ha<sup>-1</sup> equivalent: basanite (orange), peridotite (red), steel slag (purple) and glacial dust (brown) (n = 7 per treatment; for all except glacial dust n = 4).

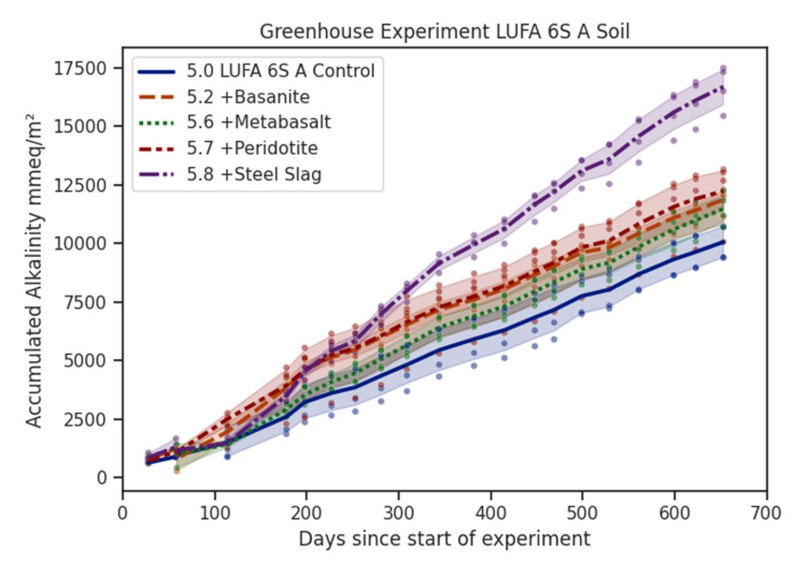




# 310 3.1.4 TA export from the clay soil "LUFA 6S"

The clayey LUFA 6S showed distinctly high alkalinity export from the control compared to the other soils described above, comparable to the export observed with Fürth 1 combined with the steel slag.

In experiment LUFA 6S A, all treatments showed a higher alkalinity export compared to their controls (Fig. 6a and b). The second experiment with LUFA 6S soil (LUFA 6S B) achieved about the same alkalinity export after only 250 days when compared with the 650 day experiment with LUFA 6S A suggesting an alkalinity production rate more than double the first experiment. The addition of limestone in the second batch resulted in comparable results to the metabasalt in the first batch.







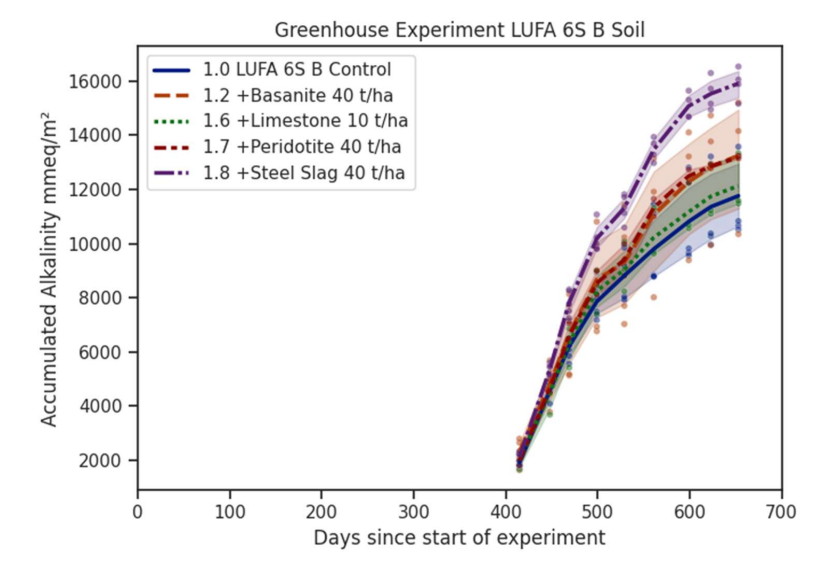


Figure 6: Accumulated leachate alkalinity results for LUFA 6S. 6a: The control treatment (blue) consisted only of the first batch A 320 of 'LUFA 6S' soil, while the other experiments included additions of EW feedstock materials at 40 t ha<sup>-1</sup> equivalent: basanite (orange), metabasalt (green), peridotite (red), and steel slag (purple) (n=4 per treatment). 6b: The control treatment (blue) consisted only of the second batch B of 'LUFA 6S' soil, while the other experiments included additions of EW feedstock materials at 10 t ha<sup>-1</sup> equivalent: limestone (green) or at 40 t ha<sup>-1</sup> equivalent: basanite (orange), peridotite (red), steel slag (purple) (n = 7 per treatment).

# 3.1.5 TA export from the loamy sand 'Fürth 2' (second batch) with commercial EW application materials

325 Experiments with the second batch of Fürth soil (Fürth 2), collected from the same field as Fürth 1, started in April 2023, with 7 feedstock materials used in commercial EW projects (Fig. 7). All treatments resulted in a higher accumulation of leachate alkalinity compared to the unamended control (Fig. 2). However, the control of the second batch of Fürth soil only reached about two thirds of the alkalinity export as the Fürth 1 soil. As observed when applying the same basanite used extensively on Fürth 1 soil to the Fürth 2 soil, we similarly saw no significant difference in leachate alkalinity between controls and treatments 330 (Fig. S4).

All commercial feedstocks produced slightly higher cumulative alkalinity than their control. EW2 (green) and EW3 (red) showed smaller increases, but remained consistently above the control. The added alkalinity fluxes ranged from 400 mmeq m $^{2}$  to 1200 mmeq m $^{2}$  and reflected a CO<sub>2</sub>-sequestration rate of  $\sim$ 0.1 to 0.3 tons per ha per year.





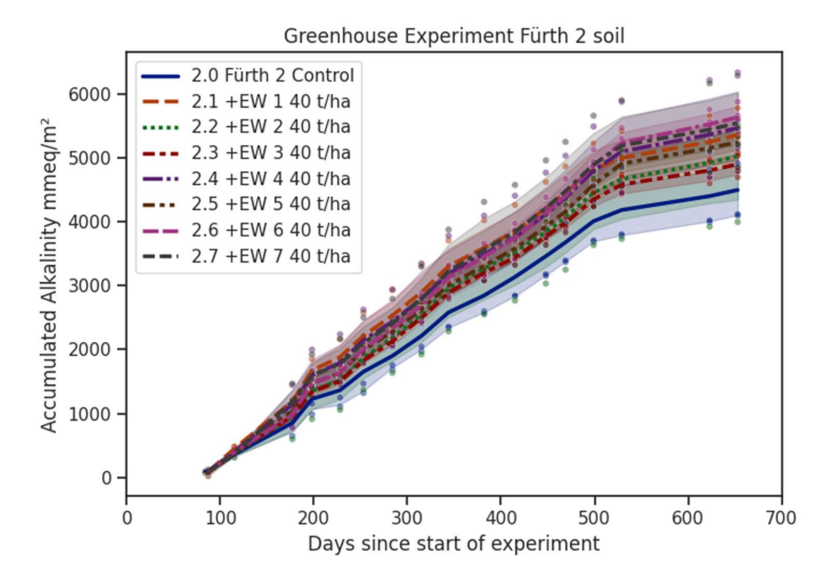


Figure 7: Accumulated leachate alkalinity results for Fürth 2 (n = 4 per treatment). The control treatment (blue) consists only of the second batch of 'Fürth' soil, while the other experiments included additions of EW feedstock materials at 40 t ha<sup>-1</sup> equivalent from different commercial companies: EW 1 to EW 7.

## 3.2 Cation pools and potential alkalinity

For the second batch experiments with LUFA 2.2 B and LUFA 6S B, the major cation contents of the 4 different soil pools (F1 exchangeable, F2 carbonate-associated, F3 oxide, F4 clay) were determined using sequential extraction after 6 and 12 months. The amount of cations that were retained in the soil were calculated as the sum of charge equivalents of Ca<sup>2+</sup>, Mg<sup>2+</sup>, Na<sup>+</sup>, and K<sup>+</sup>. Across all F1–F4 soil pools, the retained fraction of cations are substantially larger than the amount of leached alkalinity accumulated over the same time periods (Fig. 8).

At the end of an experiment, analyses of the cation pools in the control pots revealed that in the LUFA 2.2 B soil, the majority of cations are stored in the exchangeable pool (Fig. 8a). By contrast, in LUFA 6S B control, the majority of cations are stored in the carbonate and clay pools (Fig. 8b). The initial cation content of LUFA 6S B is 10 times higher than in LUFA 2.2 B, and any EW treatments to these soils results in much smaller relative changes to retained cations in LUFA 6S B than in LUFA 2.2 B

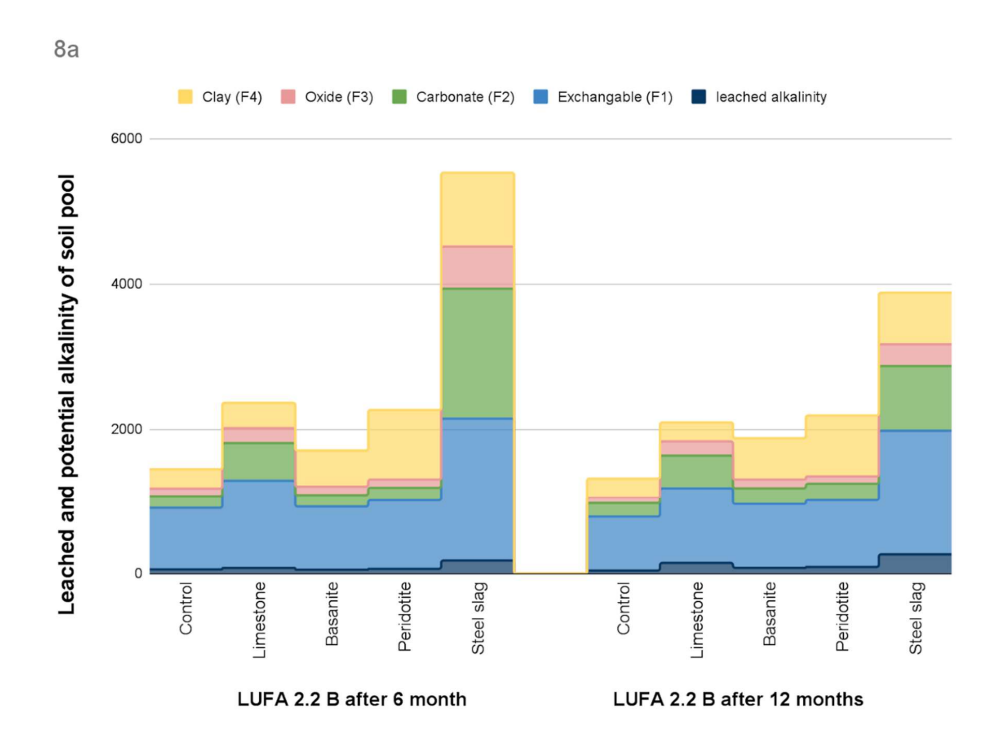
Application of 40t ha<sup>-1</sup> steel slag dose caused the largest increases in all cation pools for both soils. In LUFA 2.2 B, all 4 soil pools showed lower cation contents from 6 to 12 months after application, in, but increased leached alkalinity over the same time period. Interestingly, the sum of potential alkalinity in soil pools and leachate alkalinity decreased overall during this time. In the LUFA 6S B soil, the addition of steel slag showed slight increases in cation contents from 6 to 12 months in all soil pools, with the exception of the exchangeable pool.





Six months after a 10 t ha<sup>-1</sup> limestone dose to LUFA 2.2 B, cation contents increased in all 4 soil pools, most noticeably in the exchangeable and carbonate pools. A slight decrease in total soil cation content was observed after 12 months. By contrast, the same limestone application to LUFA 6S B resulted only in a slight cation increase in the clay pool, and negligible increases in the exchangeable and carbonate pools.

The cation content in the clay pool also increased most strongly 6 months after addition of both 40 t ha<sup>-1</sup> basanite and peridotite to the LUFA 2.2 B soil. However, application of the peridotite treatment to the LUFA 6S B soil only led to a marked increase in the clay pool after 12 months. This treatment also showed an increase in cations in the carbonate pool.







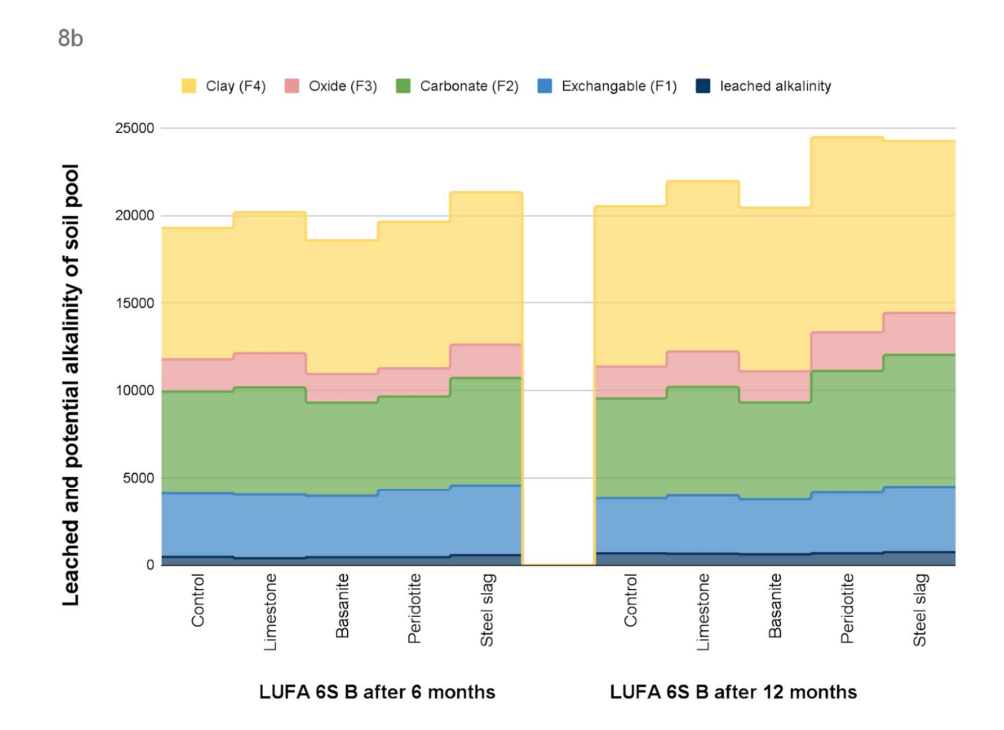


Figure 8: Sequential extraction pools and leachate alkalinity for LUFA 2.2 B (8a) and LUFA 6S B (8b). Stacked bars show cation pools from sequential extraction (F1 exchangeable, F2 carbonate-associated, F3 oxide, F4 clay). Values are the sums of charge equivalents of Ca<sup>2+</sup>, Mg<sup>2+</sup>, Na<sup>+</sup> and K<sup>+</sup> per pot (meq pot<sup>-1</sup>). Dark-blue bars in front show cumulative leachate alkalinity for the same interval (meq pot<sup>-1</sup>). (a) LUFA 2.2 B: Control, Limestone, Basanite, Peridotite and Steel-slag treatments after 6 months and after 12 months. (b) LUFA 6S B: the same treatments after 6 and 12 months.

#### 4 Discussion

# 4.1 General observed patterns

The main objective of this study was to investigate alkalinity export from soil mesocosms due to application of alkaline mineral products. The experimental results partly showed an increase, as expected. However, in some cases no measurable change between control and treated pot was observed, or even a reduction of alkalinity export was observed (Fig. 2). This unexpected result hints at potential traps for released cations within the soil system. The more detailed analysis of the different cation pools using the LUFA 2.2 and 6S soil revealed additional sinks that exceeded the added alkalinity export rates on the time scale of 6 and 12 months (Fig. 8). Such behavior has also been reported by other studies, however with fewer combinations of soil and





alkaline mineral material or for a shorter period of time (cf. McDermott et al., 2024; te Pas et al., 2025; Vienne et al., 2025). Specific processes and aspects relevant to the observed cation retardation and/or retention are discussed in more detail below.

#### 4.2 Alkalinity export and changes in soil cation pools

Across all soil types, increases in leachate alkalinity and the cation contents of different soil pools in mesocosms treated with alkaline EW feedstock materials generally reflects expected dissolution kinetics of the dominant mineral phases in each feedstock (compare Tab. S2 with Tab. S6). Steel slag, which is rich in minerals that dissolve quickly (i.e. portlandite, lime, larnite), produced the greatest increases in cation release. These cations are then mostly taken up by cation pools in the soil, including the carbonate pool. This finding is consistent with the increase in porewater alkalinity reported after adding highly alkaline industrial by-products such as steel slag and cement kiln dust in comparable core and lysimeter work (Buckingham & Henderson, 2024), as well as with kinetic parameters derived from laboratory dissolution experiments (Tab. S6) (Heřmanská et al., 2022; Heřmanská et al., 2023; Leineweber, 2002; Palandri and Kharaka, 2004; Wang et al., 1998). Calcite-bearing materials, such as metabasalt (applied at 40 t ha<sup>-1</sup>) and limestone (applied at 10 t ha<sup>-1</sup> to LUFA 2.2 B and LUFA 6S B; see Tab. S2 for mineral/TIC composition), produced the second strongest alkalinity gains relative to controls, with the clearest responses in acidic soils. Peak effects were observed for metabasalt in LUFA 2.1 (+369 % at day 650) and LUFA 2.2 390 A (+186 % by day 250), and for limestone in LUFA 2.2 B (+175 % by day 250) (Fig. 2). The metabasalt alkalinity signal compared to the control decreased from 186 % after 250 days to ~130 % by day 650 (Fig. 2). This finding is consistent with rapid early dissolution of abundant calcite, followed by slower weathering with increasing pH (compare Fig. 5 with Fig. S7). In more alkaline soils, the effect of adding a calcite-bearing feedstock to alkalinity was small or negative (e.g. LUFA 6S A ~114 %; Fürth 1 ~72 %). Overall, the strong responses under acidic conditions and the reduced impacts at higher pH align with established liming behavior and buffering constraints (Barber, 1984; Buckingham and Henderson, 2024; Goulding, 2015; Hamilton et al., 2007; Nye and Ameloko, 1987). Similar trends were also found for carbonate-rich crushed returned concrete (McDermott et al., 2024).

The observation that alkaline soils may generate lower relative alkalinity export may be explained by high Ca-release from calcite-bearing feedstocks promoting carbonate formation in the soils as saturation limits are reached, and pH-related dissolution dynamics becoming slower. The increase observed in the carbonate cation pool supports the explanation of active carbonate formation (Fig. 8). Steel slag treatments also showed significant increases in other cation pools such as the exchangeable, clay and oxide pools. They all exceed the alkalinity export flux for both examined soils after 12 months, as observed elsewhere (cf. Maxbauer et al., 2025).

405 Peridotite (Fig. 2, red) addition resulted in modest alkalinity gains, with the strongest responses in acidic soils. In LUFA 2.1 and LUFA 2.2 A, leachate alkalinity rose to 199 % and 240 % respectively, when compared to the control by day 650. Notably, LUFA 2.2 A showed opposite dynamics to the metabasalt: peridotite fell to 85 % at day 250, but then increased to 240 % by day 650, whereas metabasalt peaked early (186 % at day 250) and declined thereafter (130 % at day 650). In LUFA 2.2 B (250

https://doi.org/10.5194/egusphere-2025-5402 Preprint. Discussion started: 24 November 2025 © Author(s) 2025. CC BY 4.0 License.



420



days), alkalinity export by peridotite reached only 110 % relative to the control. This finding is consistent with a slow early change in batch A of LUFA 2.2. In neutral to alkaline substrates, effects were weak or negative, with LUFA 6S soils at 112–144 % and Fürth 1 at 77 % when compared to their controls.

Similar to carbonate-bearing feedstocks, peridotite additions showed a clear soil pH relationship with increasing leachate alkalinity. However, the response was slower due to its mineral weathering kinetics. Specifically, Peridotite (79 % olivine) produced modest to moderate alkalinity gains in acidic soils that intensified over two years (cf. Amann et al., 2020; te Pas et al., 2025; Ten Berge et al., 2012), but caused little or even negative responses in neutral to alkaline soils (Oelkers et al., 2018; Pokrovsky and Schott, 2000) (Fig. 2). These trends are consistent with both the slower dissolution kinetics of olivine, (which has an up to 4 orders of magnitude lower dissolution rate than calcite; Tab. S6 (Heřmanská et al., 2023; Leineweber, 2002)), and with the retention of Mg<sup>2+</sup> in soils or secondary phases (cf. Iff et al., 2024; te Pas et al., 2025).

Basanite (Fig. 2, orange) yielded the weakest leachate alkalinity responses, typically near control levels (84–142 %), across both acidic and more alkaline soils. This reduced signal is consistent with its pyroxene-rich and olivine-poor mineralogy, and thus slower weathering rates compared to the peridotite. These results also agree with other studies that show a substantial fraction of alkalinity can remain retained in the soil matrix for months to years (Amann et al., 2022; Buckingham and Henderson, 2024; Holden et al., 2024; Kelland et al., 2020; Vienne et al., 2022). Such retention can become especially strong when water supply is limited or when preferential flow bypasses reactive zones (cf. Amann et al., 2020).

Overall, the results support a consistent hierarchy in leachate alkalinity increase that reflect soil pH influenced dissolution kinetics: steel slag > carbonate-rich rocks > peridotite > basanite. Alkalinity export is likely also strongly enhanced by initial carbonate-driven pulses in acidic soils (Fig. 9). Notably, the felsic glacial rock dust, despite containing slower-dissolving silicate minerals (35 % plagioclase, 28 % mica, 14 % amphibole, 12 % quartz), generated leachate alkalinity on a scale comparable to the 10 t ha<sup>-1</sup> limestone treatment (Fig. 2). This outcome reflects its much finer grain size and correspondingly distinctly larger reactive surface area (Tab. S3).

#### 4.3 Soil properties affecting leachate alkalinity

Our findings generally support the expectation that acidic conditions accelerate alkaline feedstock dissolution (Hartmann et al., 2013; Palandri and Kharaka, 2004; Renforth et al., 2015). They also support a lower initial soil pH being a key factor for generating leachate alkalinity through enhanced weathering (Fig. 9). The strongest relative alkalinity responses were observed in acidic soils such as LUFA 2.1 (pH 4.6) and LUFA 2.2 (pH 5.5), especially when treated with carbonate-bearing rocks or highly alkaline materials. The acidic sand LUFA 2.1, for example, showed notable high increases (+++) when compared to the control. This effect was even stronger when treated with carbonate-bearing rocks and highly alkaline materials (Fig. 9).





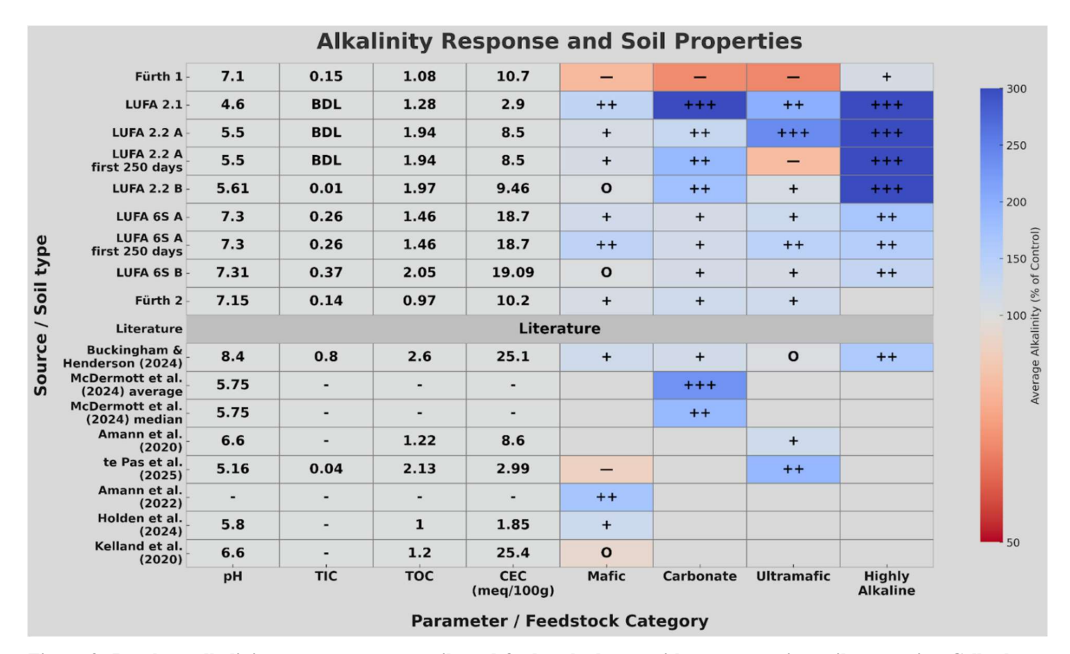


Figure 9: Leachate alkalinity responses across soils and feedstock classes with accompanying soil properties. Cells show average leachate alkalinity relative to the untreated control (% of control; color scale centered at 100 %) for four feedstock categories (Mafic, Carbonate, Ultramafic, Highly alkaline). Blue tones indicate values above the control (greater alkalinity release), red tones less than the control. Symbols summarise effect size: — (<95 %), O (95–105 %), + (105–125 %), + + (125–200 %), +++ (>200 %). The four left columns report initial pH, TIC, TOC, and CEC (meq/100g) for each soil. The 'Literature' band separates our greenhouse results (upper block) from values compiled from selected published studies (lower block). BDL = below detection limit; '-' = not reported.

By contrast, soils with an initial neutral to alkaline pH (e.g. Fürth 1 at pH 7.1, LUFA 6S at pH 7.3 and Fürth 2 at pH 7.15) generally showed weaker or even negative relative leachate alkalinity responses compared to the control, regardless of feedstock. Although experiments with feedstocks on LUFA 6S showed high absolute alkalinity export, this may not necessarily be due to weathering of feedstock, but rather background soil buffering or more intense dissolution of pre-existing soil carbonates (as indicated by the high CEC and TIC values).

This finding warrants a closer examination of the processes responsible for generating alkalinity in LUFA 6S. The rapid and early differentiation of alkalinity between the treated and control pots in LUFA 6S (within 200 days, especially in LUFA 6S B within 100 days) contrasts sharply with the delayed response in LUFA 2.1 and LUFA 2.2 soils (e.g. LUFA 2.2 + ultramafic after 350 days and LUFA 2.2 + mafic after 650 days) (Fig.6). Given the higher initial pH (>7.3) and the presence of more soil inorganic carbon (SIC) in LUFA 6S, this phenomenon raises a crucial question: why does a soil with a high initial pH and the presence of SIC (whose dissolution kinetics are faster than those of the added silicate minerals) exhibit an earlier and more pronounced increase in leachate alkalinity between control and treatment? We propose two scenarios to explain the early increase in alkalinity in LUFA 6S. These show that the magnitude and timing of the response is not only necessarily dictated





by mineralogical composition or proton activity, but also hydrological residence time, reactive surface area, precipitation of secondary phases,  $pCO_2$  and biological activity. Examination of such other factors might shed more light on the increase in alkalinity caused by a specific feedstock within a specific soil. In addition, soil models, as suggested by Kanzaki et al. (2022) and Bertagni et al. (2025) calibrated for such conditions might help to explain the main steering factors.

## 4.3.1 Potential Scenarios for Early Alkalinity in high-pH Soils

1. Cation exchange dynamics and pre-existing carbonates: Cation-anion diagrams of leached cations and anions for LUFA 6S B (Fig. S3) consistently show  $Ca^{2+}$  as the dominant cation exiting the system. About 6 months into the experiment, a clear increase in leachate  $Ca^{2+}$  concentration for the treatments compared to the control emerges and persists. This differs from observations in LUFA 2.2 B soils, where  $Ca^{2+}$  is also the main cation in the leachate water, but the addition of mafic material (basanite) leads to an increase of the percentage of leached  $Na^{+}$  (from nepheline dissolution) relative to the control over time, in addition to elevated  $Mg^{2+}$  (from forsterite dissolution) from the application of ultramafic material (peridotite) (Fig. S2). In a high-pH soil such as LUFA 6S, which has an inherently elevated carbonate background, CEC sites are likely to be occupied with  $Ca^{2+}$  ions due to the natural weathering of its own carbonates-bearing soil (Taalab et al., 2019).

The presence of pre-existing carbonates (Tab. S1) and cation exchange dynamics is evident in LUFA 6S due to the steep increase in leachate alkalinity. These dynamics involve the exchange of cations between the soil and the surrounding environment. When a new rock feedstock is added, other cations are released via weathering (mostly Mg<sup>2+</sup>), which then displace the pre-existing Ca<sup>2+</sup> from the CEC sites in a competitive process (Sparks et al., 2022). The displaced Ca<sup>2+</sup> then contributes to the observed increase in leachate alkalinity.

2. Enhanced dissolution of pre-existing soil carbonates: The second scenario suggests that the pre-existing carbonates in the LUFA 6S are playing a more direct role in the observed increase in alkalinity. Since our added mafic material contains no carbonates and its Ca-bearing silicate minerals are not expected to weather as quickly as the nepheline in a high-pH environment when compared to the LUFA 2.2 soils, it is possible that the pre-existing soil carbonates are dissolving more quickly (Tab. S6) (Heřmanská et al., 2022, Heřmanská et al., 2023; Leineweber, 2002; Pokrovsky and Schott, 2000; Wang et al., 1998). This accelerated dissolution could be a consequence of subtle changes in leachate water chemistry or enhanced biological activity induced by the addition of the feedstock. For example, increased microbial respiration could lead to greater CO<sub>2</sub> release and the formation of carbonic acid, or stimulate the production of organic acids (Fig. S5) (Cristina Moscatelli et al., 2024; Gocke et al., 2011; Goll et al., 2021; Rineau et al., 2025). These acid-producing processes would enhance the dissolution of existing carbonates, thereby contributing to the faster increase in alkalinity observed in LUFA 6S compared to the control and later increases in alkalinity in LUFA 2.2 soils.

It is possible that a combination of both scenarios contributes to the observed phenomena. Comparable increases in alkalinity in high pH, carbonate-bearing soils with similar cation exchange capacity values to LUFA 6S have been reported by Buckingham and Henderson (2024). While they applied basalt with a higher calcium mineral content, the exclusive origin of

https://doi.org/10.5194/egusphere-2025-5402 Preprint. Discussion started: 24 November 2025 © Author(s) 2025. CC BY 4.0 License.





the observed calcium and alkalinity from weathered basalt may warrant further investigation. Much like our findings, theirs could indicate that some of the observed calcium and alkalinity is derived from exchangeable pools and pre-existing carbonates, rather than exclusively from the added silicate feedstock. This suggests that the rapid increase in alkalinity in highph, carbonate-rich soils may be a more general phenomenon, influenced by cation exchange dynamics and enhanced carbonate dissolution, irrespective of the mineralogy of the added feedstock. Further research is required to quantify the contributions of these proposed mechanisms to the overall alkalinity budget in such complex soil systems.

# 500 4.3.2 Permeability and LUFA reproducibility

Having focused on the properties and interactions of different soils and rocks in the context of EW, the question remains as to whether these are the only factors controlling the performance of dissolving EW feedstocks and creating increases in alkalinity. The accumulated alkalinity from an outdoor lysimeter experiment using Fürth soil (Fig. 10; (Paessler et al., 2025)) was affected by rain events and droughts. Early in the experiment (<100 days), an intense rainfall following a dry spell produced a pronounced flushing event that contributed ~25 % of the total alkalinity export measured across the entire 850 day monitoring period. Despite temporary heat events in the greenhouse during this study's experiments, such variability in water abundance did not occur due to the relatively high artificial watering rates that were further increased during heat waves. Although the rate curves for alkalinity production over time are much smoother in the greenhouse experiments presented here (Fig. 3-7), they still reflect a generally higher flux around day 100 to 200. Therefore, it cannot be ruled out that the accelerated production of alkalinity at the beginning of an enhanced weathering experiment may be due to mixing (homogenisation) and setting up the experiment induced microbial activity after rewetting (the so-called Birch effect) (Birch, 1958). Comparable behaviour a few weeks after experimental initiation has also been identified in other EW column experiments (cf. Amann et al., 2022; Vorrath et al., 2025).





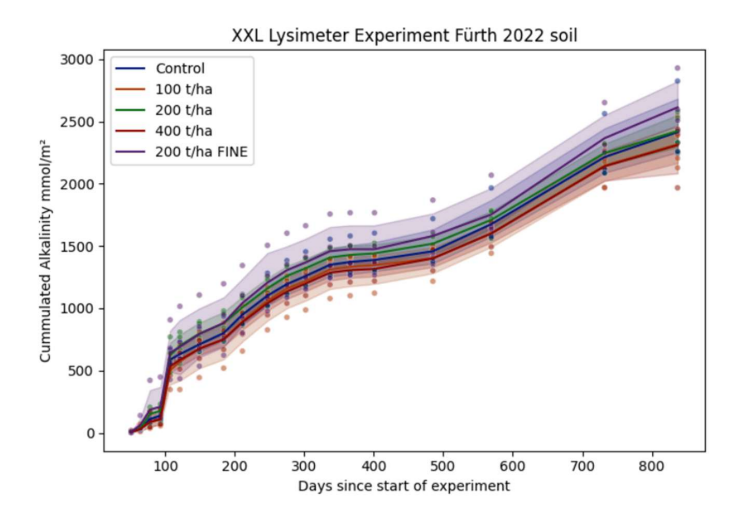


Figure 10: Data from an outdoor mesocosm experiment with different basanite application rates and grain sizes affected by seasonal variations of rainfall (Paessler et al., 2025).

Despite using homogenised, standardised soils from the agricultural research and investigation institute LUFA Speyer, the two batches of the same LUFA soils behaved quite differently in the greenhouse. The 2024 batches (LUFA 2.2 B and LUFA 6S B) consistently produced more alkalinity per litre of leachate in a shorter period of time than the 2023 batches, irrespective of the feedstocks, (we added the equivalent of 40 t ha<sup>-1</sup> of metabasalt containing 27 % calcite in 2023, and 10 t ha<sup>-1</sup> of limestone containing 85 % calcite in 2024). As further expanded on further down we attribute this primarily to longer pore-water residence times and a stronger initial acid supply in the experiments that started later. The relative soil-feedstock driven trends for generated alkalinity, however, do not change much between the different batches (Fig.9).

First, despite efforts to ensure comparable properties and grain-size distributions of soil, the 2024 batch of the standardised soils differed in their fine fraction, had a lower initial moisture content, and exhibited visible swelling upon initial wetting. The swelling of clay-rich minerals reduces macroporosity and near-saturated hydraulic conductivity, shifting flow from preferential to matrix-dominated pathways and increasing residence time. This is consistent with studies on expansive/smectitic clays that demonstrate alteration of pore architecture by wetting-induced swelling decreases hydraulic conductivity (Shainberg et al., 2001). This means that pore waters carry more DIC/alkalinity per unit outflow. This hydrological control of weathering fluxes is also a key finding of reactive-transport frameworks (Maher, 2010; Maher and Chamberlain, 2014).

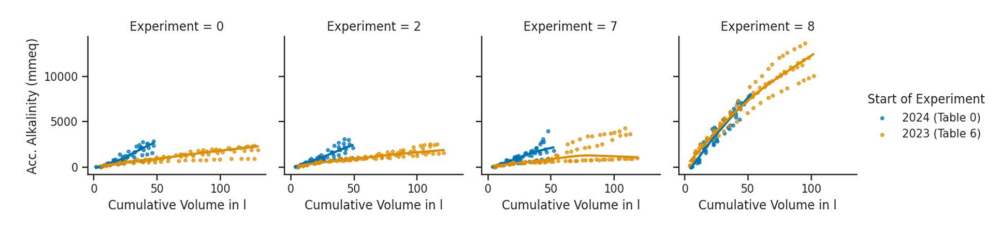
Second, a pronounced dry–rewet ("Birch") pulse at the onset of irrigation in 2024 likely elevated soil-gas pCO<sub>2</sub> due to mineralisation of soil organic matter, and compaction-induced reductions in pore connectivity (lower gas diffusivity) would have helped sustain these elevated concentrations (Fig. S5) (Birch, 1958; Smith et al., 2023). Rewetting dry soil triggers rapid microbial resuscitation and CO<sub>2</sub> bursts (Smith et al., 2023), potentially accelerating the dissolution of carbonates within the





soil (LUFA 6S B) or Ca/Mg-bearing silicates (LUFA 2.2 B) in a non-saturated environment. This is consistent with the steeper slopes in cumulative alkalinity versus cumulative volume for the later batches (Fig. 11).





540

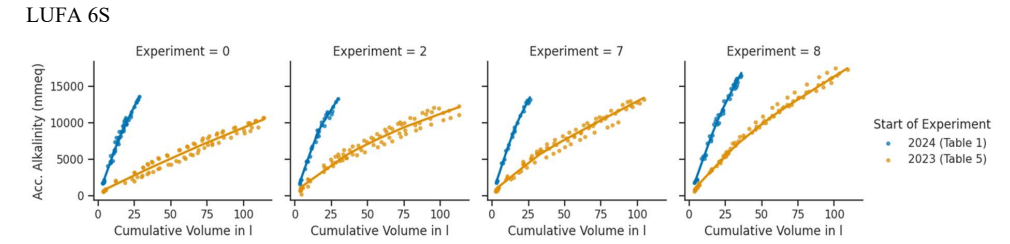


Figure 11: Accumulated alkalinity export (y-axis) vs. cumulative leachate volume (x-axis) for LUFA soils (starting in 2023 vs. 2024).

Two rows of figures compare LUFA 2.2 (top) and LUFA 6S (bottom) across experiments 0 (control), 2 (basanite), 7 (peridotite), and 8 (steel slag). Within each soil, colours denote the two batches started with different initial water contents: orange = batch A started 2023 (wetter start), and blue = batch B started 2024 (drier start). Water-holding capacities (determined by LUFA after DIN EN ISO 14240-2:2011-09): LUFA 2.2 A: 26.7 % (initiated 2023), B: 19 % (initiated 2024); LUFA 6S A: 26.47 % (initiated 2023), B: 17.96 % (initiated 2024).

# 550 4.4 Cation pools and the significance of their temporal evolution

In line with previous studies (e.g. Iff et al., 2024; te Pas et al., 2025; Pogge von Strandmann et al., 2022b; Vienne et al., 2025), which emphasise the retention of weathering products within the soil matrix (secondary minerals or cation exchange sites), our data provide the opportunity to understand to what extent feedstocks actually weather, and what happens to cations within the soils after mineral dissolution. Importantly, the dominance of in-soil storage also emerges in this study in the comparison of cation content of soil chemical pools with leached alkalinity. In many cases, the treatment–control differences across the four sequential-extraction pools substantially exceed the corresponding differences in leached alkalinity (Fig. 8; Tab. 3). Note that negative treatment–control values yield ratios < 0; thus to avoid artefacts driven by very small negative denominators, these cases are reported simply as "< 0" (Tab. 3 and 4).



580

585



Given soil heterogeneity and single-pot uncertainty, we focus the remainder of the discussion on the main trends. Below, we compare the two soils on which sequential extraction was performed in terms of pH, cation exchange capacity, carbonate background and the fate of weathering products over time.

In the acidic, non-calcareous, sandy loam LUFA 2.2 B (pH ≈ 5.3, CEC ≈ 9.5 meq (100 g)<sup>-1</sup>, no background SIC), the relative export of alkalinity increases over time (control relative to treatment), accompanied by an increase of cations in the exchangeable (F1) and carbonate-associated (F2) pools, and a decrease of the soil pool/ leachate ratio (Tab. 3). This trend is consistent across all treatments. The alkalinity export for steel slag was intense from the very beginning of the experiment, however it took more time for limestone to show alkalinity increase in the leachate, and even longer for peridotite and basanite (Figure 5b). This is reflected by changes in both soil cation to leachate alkalinity ratios, and specific cation ratios (Tab. 3 and 4), indicative of preferential cation release due to weathering of specific minerals in each feedstock. For instance, Ca<sup>2+</sup> is preferentially released by the weathering of limestone/steel slag, Na<sup>+</sup> and K<sup>+</sup> by the basanite, and Mg<sup>2+</sup> from the forsterite in peridotite (Fig. 12 a). In this acidic soil type, cations held in the exchangeable and carbonate-associated pools of the steel slag and limestone treatments decrease between 6 and 12 months, while the oxide and clay pools do not increase significantly. Meanwhile, alkalinity continues to be exported in leachate. This trend is also visible in the decline in the in-soil pool build-up to leached alkalinity ratio (Tab. 3). Despite this trend, a factor of 10 times more alkalinity equivalents are still retained in soil phases (Tab. 4).

In the carbonate-bearing LUFA 6S B (pH 7.3, CEC 19.1 meq (100 g)<sup>-1</sup>, SIC 0.37 wt%), alkalinity is also leached; however, only a limited fraction is derived directly from feedstock dissolution. Most of the exported alkalinity appears to originate from background soil carbonate dissolution, as indicated by several indices:

- 1. The size of the carbonate pool of cations decreases after basanite and peridotite treatment, especially after 6 months (Fig. 8/ Fig. S6 and Fig. 12b).
  - 2. Limestone application does not increase the leaching of alkalinity relative to the control; in fact, alkalinity export is the lowest of all treatments (Tab. 3 & 4; Fig. 6).
- 3. An increase in the F4 (clay) pool, alongside both an increase in mineral specific cations (Na<sup>+</sup> for basanite and Mg<sup>2+</sup> for peridotite), as well as an increase in soil cations to leachate alkalinity ratio over time, show weathering of the added feedstocks, and contribution to the clay pool. Concurrently, the exchange complexes are gradually depleted and secondary phases (F2–F4) accumulate, which is consistent with longer residence times and strong buffering in this high-pH, high-CEC soil.
- 590 Overall, these patterns suggest that the addition of rock to LUFA 2.2 B primarily results in the direct export of alkalinity and initial loading and releasing of the exchangeable and carbonate-associated pools. By contrast, in LUFA 6S B, the addition of rock mainly mobilises and re-partitions soil-derived cations into secondary carbonates and clay/organometallic associations,





with limited immediate export. We note that single-pot replication introduces variability in absolute magnitudes, but the first-order trends and mineral-specific cation signals are consistent across the datasets.

595

		LUFA 2.2 B			LUFA 6S B		
		soil pools	Leached	soil pools /	soil pools	Leached	soil pools /
		(meq)	alkalinity (meq)	TA leached	(meq)	alkalinity (meq)	TA leached
	Control	1,449	57	26	19,285	459	42
	Limestone	2,363	76	31	20,177	385	52
6 months	Basanite	1,707	52	33	18,568	441	42
	Peridotite	2,265	64	36	19,637	441	45
	Steel slag	5,530	179	31	21,322	556	38
12 months	Control	1,321	40	33	20,522	661	31
	Limestone	2,093	146	14	21,957	638	34
	Basanite	1,877	77	24	20,435	608	34
	Peridotite	2,189	89	25	24,466	662	37
	Steel slag	3,878	264	15	24,242	728	33

Table 3: Absolute partitioning of cations between soil storage and leachate export for two soils (LUFA 2.2  $^{\circ}$ B, LUFA 6S  $^{\circ}$ B) after 6 and 12 months. For each treatment, we report: (i) soil pools (meq pot<sup>-1</sup>)' = the total potential alkalinity stored in the soil of one pot, computed as the sum of charge equivalents of Ca<sup>2+</sup>, Mg<sup>2+</sup>, Na<sup>+</sup>, and K<sup>+</sup> across the sequential-extraction pools (F1 exchangeable + F2 carbonate-associated + F3 oxide + F4 clay); (ii) 'Leached alkalinity (meq)' = the cumulative alkalinity exported in leachate over the same period; and (iii) 'soil pools / TA leached' = the absolute storage-to-export ratio, indicating how large the in-soil cation inventory is relative to what was exported.

605

610





		LUFA 2.2 B			LUFA 6S B		
ļ		Δ soil pools	Δ leached	Δ soil pools /	$\Delta$ soil pools	Δ leached	$\Delta$ soil pools /
		(meq)	alkalinity (meq)	Delta TA leached	(meq)	alkalinity (meq)	Δ TA leached
	Limestone	895.7	19.25	46.53	965.6	-73.40	<0
	Basanite	263.0	-4.80	<0	-698.9	-18.05	<0
6 months	Peridotite	809.5	7.25	111.65	369.4	-18.05	<0
	Steel slag	3,959.0	122.75	32.25	1,939.5	97.50	19.89
	Limestone	666.5	105.90	6.29	1,457.8	-22.90	<0
	Basanite	518.1	37.30	13.89	-33.3	-52.95	<0
	Peridotite	818.7	49.35	16.59	3,942.6	1.20	3,285.52
	Steel slag	2,333.2	223.85	10.42	3,653.2	67.40	54.20

Table 4: Partitioning of treatment-derived cations between soil storage (sequential-extraction pools) and leachate export for two soils (acidic LUFA 2.2 B, slightly alkaline LUFA 6S B) at 6 and 12 months. For each treatment, three quantities are reported: (i)  $\Delta$  four pools = (treatment – control) summed across F1 exchangeable + F2 carbonate-associated + F3 oxide + F4 clay (meq pot<sup>-1</sup>); (ii)  $\Delta$  leached alkalinity = (treatment – control) cumulative leachate alkalinity (meq pot<sup>-1</sup>); and (iii) the partitioning ratio = ( $\Delta$  four pools)  $\div$  ( $\Delta$  leached alkalinity).





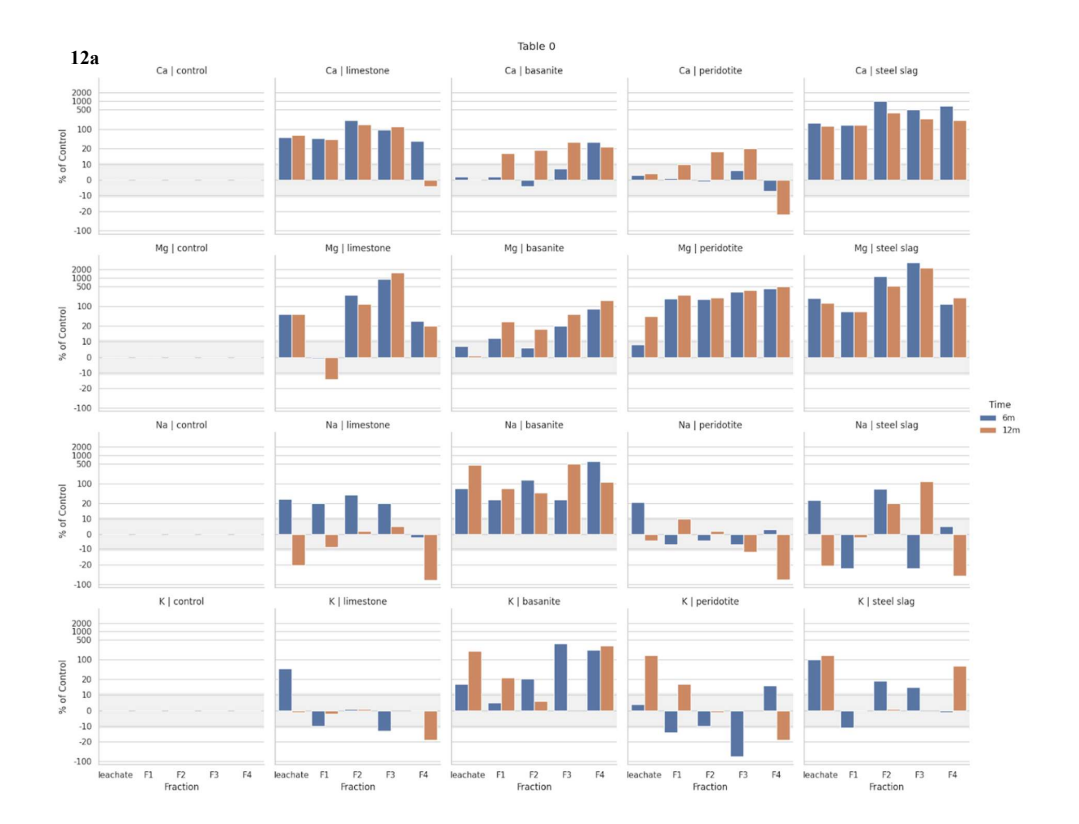








Figure 12: Relative cation partitioning by treatment, time, and pool for acidic LUFA 2.2 B (12a) and slightly alkaline LUFA 6S B (12b). Panels are arranged by ion (rows:  $Ca^{2+}$ ,  $Mg^{2+}$ ,  $Na^+$ ,  $K^+$ ) and treatment (columns: control, limestone, basanite, peridotite, steel slag). Within each panel, bars show the percentage of the control for each pool on the x-axis: leachate (cumulative export over the interval) and the four sequential-extraction pools—F1 exchangeable, F2 carbonate-associated, F3 oxide (Fe/Mn-oxide bound), and F4 clay. Colors indicate sampling time (blue = 6 months, orange = 12 months). The y-axis ('% of control') is centered at 0 %; 100 % denotes parity with the control, values >100 % indicate enrichment relative to the control, and <0 % indicates depletion.

# 5. Conclusion

Our results demonstrate that the extent and fate of enhanced weathering (EW) products are significantly influenced by soil characteristics, even under tightly controlled conditions. Beyond mineralogy, the factors that exert a first-order control on both dissolution and the partitioning of released cations include soil pH, cation exchange capacity, the presence of soil inorganic carbon and hydrogeological properties (e.g. permeability and flow regime). Dry—wet cycles, especially immediately after feedstock mixing/application, have a significant impact on early fluxes and experimental reproducibility. Crucially, it was only through experiments spanning longer than several months that these patterns became evident highlighting the need for longer duration studies to avoid pre-emptive conclusions biased by transient effects.

https://doi.org/10.5194/egusphere-2025-5402 Preprint. Discussion started: 24 November 2025 © Author(s) 2025. CC BY 4.0 License.





- The mineralogical composition and dissolution kinetics of the feedstock can be leveraged to increase overall efficacy of alkalinity export. At the same time, particle size and specific surface area offer additional opportunities for improvement, as demonstrated by an experiment involving ultrafine felsic glacial sediment. Realising the gains of such a fine material will require systematic, comparable trials to determine the extent to which optimisation remains compatible with life-cycle assessment (LCA) constraints (e.g., grinding energy and logistics).
- Across all soils investigated, in-soil retention of base cations dominates over leachate export. The extent to which this occurs varies depending on the soil type. After one year, the feedstock that yielded the greatest alkalinity export via leachate from an acidic sandy loam (steel slag) retained approximately 10 times more cation charge equivalents in solid pools than exported as alkalinity. By contrast, a clay soil with a trace carbonate background retained approximately 54 times more in solid pools. This difference supports the notion that in acidic, low-CEC soils, a greater proportion of alkaline mineral weathering results is exported in leachate as alkalinity. This is consistent with observations from other acidic/low-buffer systems (e.g. lateritic soil; Amann et al., 2022). By contrast, the prominent increase of the clay (F4) pool in high-pH clay-rich, carbonate-bearing soil suggests that cations released by weathering are preferentially stabilised within clay associations, preventing alkalinity export to drainage.
- Our results show that cation partitioning in soil chemical pools is a critical component of calculations for the efficacy of EW, and the data we present can be used to benchmark models against. While these data suggest that only some of the theoretical CDR potential of EW feedstocks is realised within practical timescales, broader sequential extraction campaigns across a wider range of soils and feedstocks are needed. These need to be combined with further targeted analyses of organic matter composition, to test whether mineral dissolution promoted clay formation stabilises organic matter and creates a transient organic sink, which could mean CDR without an increase in leachate TA.
- Alkalinity generation and export is not only a function of the feedstock composition, but of soil type. It therefore remains necessary to study the dynamics of soil cation pools with time, their response to chemical and hydrological changes, and their role in alkalinity export. This should be done across diverse rock/soil combinations to identify which combinations may constitute long-term carbon sinks and is a vital step that is needed before accurate predictive models can be built for enhanced weathering applications.

#### 660 Data availability

Data supporting and used within this study are available at GitHub:

(https://github.com/dirkpaessler/carbdown\_greenhouse\_2023\_2024) and archived for citation via Zenodo (https://doi.org/10.5281/zenodo.17492773).

https://doi.org/10.5194/egusphere-2025-5402 Preprint. Discussion started: 24 November 2025

© Author(s) 2025. CC BY 4.0 License.





#### **Author contributions**

665 JH, RS, MH, JSH and DP planned and designed the experiments; AS, TR, BC, JB and JSH performed the measurements; JSH, DP, TL, AV and JH analysed the data; JSH and JH wrote the manuscript draft; JH, JB, TL, IS, MH, PPvS, TR, BC, AV, AS, RS and DP reviewed and edited the manuscript.

## Competing interests

Mathilde Hagens is a member of the editorial board of Biogeosciences.

670 The authors declare that this research was funded entirely by the Carbon Drawdown Initiative (CDI), a privately funded German company that has not yet made a profit and is solely financed by co-author Dirk Paessler (CDI's CEO and owner). Mr Paessler has also invested high-risk philanthropic capital in 33 carbon dioxide removal (CDR) start-ups (approximately half of which are focused on enhanced weathering and none of which are currently profitable). He holds three personal patents related to enhanced weathering that are unrelated to the methods or findings of this paper. Seven enhanced weathering companies (including some in which the CDI has investments) donated small quantities of rock dust for the study, but did not provide any financial support or play a role in the research design or analysis. No CDI-affiliated author holds an advisory or board position in these companies. The paper does not endorse any specific company or technology; instead, it advocates further experimentation and a cautious approach to the commercialisation of enhanced weathering. Tom Reershemius and Bruno Casimiro acknowledge receiving separate research funding from UNDO Carbon that did not contribute to this work. No benefits for UNDO Carbon were generated by this work.

# Acknowledgement

We thank the Paessler family foundation for spending money on philanthropic work and the support of the Carbon Drawdown Initiative. We also thank everybody who helped and supported us with the built up and maintenance of the greenhouse experiment including: Anna Paessler, Christina Schubert, Maria-Elena Vorrath, Mariola Szyrlewski, Monika Müller, Tanja Wartenberg, Jakob Rietzler, Jelle Bijma, Johannes Meyer zu Drewer, Jonas Scholz, Jörn Paessler, Lukas Rieder, Patrick Niedermayer, Philip Tillmanns, Robert van Geldern, Thorben Amann, Tim Hauke, Xuming Li. Al has been used to generate ideas for table layouts and grammatical formulations.

#### References

Almaraz, M., Bingham, N. L., Holzer, I. O., Geoghegan, E. K., Goertzen, H., Sohng, J., and Houlton, B. Z.: Methods for determining the CO2 removal capacity of enhanced weathering in agronomic settings, Front. Clim., 4, https://doi.org/10.3389/fclim.2022.970429, 2022.





- Amann, T., Hartmann, J., Hellmann, R., Pedrosa, E. T., and Malik, A.: Enhanced weathering potentials—the role of in situ CO2 and grain size distribution, Front. Clim., 4, https://doi.org/10.3389/fclim.2022.929268, 2022.
- Amann, T., Hartmann, J., Struyf, E., de Oliveira Garcia, W., Fischer, E. K., Janssens, I., Meire, P., and Schoelynck, J.:
- 695 Enhanced Weathering and related element fluxes a cropland mesocosm approach, Biogeosciences, 17, 103–119, https://doi.org/10.5194/bg-17-103-2020, 2020.
  - Bandara, U. G. C., Diyabalanage, S., Barth, J. A. C., and Chandrajith, R.: Recharging Mechanisms and Seawater Intrusion in Karst Aquifers in Northwest Sri Lanka, Based on Hydrogeochemistry and Water Isotopes, ACS EST Water, 3, 1678–1686, https://doi.org/10.1021/acsestwater.2c00454, 2023.
- 700 Barber, S. A.: Liming Materials and Practices, in: Soil Acidity and Liming, John Wiley & Sons, Ltd, 171–209, https://doi.org/10.2134/agronmonogr12.2ed.c4, 1984.
  - Beerling, D. J., Kantzas, E. P., Lomas, M. R., Wade, P., Eufrasio, R. M., Renforth, P., Sarkar, B., Andrews, M. G., James, R. H., Pearce, C. R., Mercure, J.-F., Pollitt, H., Holden, P. B., Edwards, N. R., Khanna, M., Koh, L., Quegan, S., Pidgeon, N. F., Janssens, I. A., Hansen, J., and Banwart, S. A.: Potential for large-scale CO2 removal via enhanced rock weathering with croplands, Nature, 583, 242–248, https://doi.org/10.1038/s41586-020-2448-9, 2020.
  - Berner, R. A.: The long-term carbon cycle, fossil fuels and atmospheric composition, Nature, 426, 323–326, https://doi.org/10.1038/nature02131, 2003.
  - Berner, R. A., Lasaga, A. C., and Garrels, R. M.: Carbonate-silicate geochemical cycle and its effect on atmospheric carbon dioxide over the past 100 million years, Am J Sci U. S., 283:7, https://doi.org/10.2475/ajs.283.7.641, 1983.
- 710 Bertagni, M. B., Calabrese, S., Cipolla, G., Noto, L. V., and Porporato, A.: Advancing Enhanced Weathering Modeling in Soils: Critical Comparison With Experimental Data, J. Adv. Model. Earth Syst., 17, e2024MS004224, https://doi.org/10.1029/2024MS004224, 2025.
  - Birch, H. F.: The effect of soil drying on humus decomposition and nitrogen availability, Plant Soil, 10, 9–31, https://doi.org/10.1007/BF01343734, 1958.
- Buckingham, F. L. and Henderson, G. M.: The enhanced weathering potential of a range of silicate and carbonate additions in a UK agricultural soil, Sci. Total Environ., 907, 167701, https://doi.org/10.1016/j.scitotenv.2023.167701, 2024.
  Buss, W., Hasemer, H., Sokol, N. W., Rohling, E. J., and Borevitz, J.: Applying minerals to soil to draw down atmospheric carbon dioxide through synergistic organic and inorganic pathways, Commun. Earth Environ., 5, 602, https://doi.org/10.1038/s43247-024-01771-3, 2024.
- 720 Clarkson, M. O., Larkin, C. S., Swoboda, P., Reershemius, T., Suhrhoff, T. J., Maesano, C. N., and Campbell, J. S.: A review of measurement for quantification of carbon dioxide removal by enhanced weathering in soil, Front. Clim., 6, https://doi.org/10.3389/fclim.2024.1345224, 2024.
  - Fuss, S., Lamb, W. F., Callaghan, M. W., Hilaire, J., Creutzig, F., Amann, T., Beringer, T., de Oliveira Garcia, W., Hartmann, J., Khanna, T., Luderer, G., Nemet, G. F., Rogelj, J., Smith, P., Vicente, J. L. V., Wilcox, J., del Mar Zamora Dominguez, M.,





- and Minx, J. C.: Negative emissions—Part 2: Costs, potentials and side effects, Environ. Res. Lett., 13, 063002, https://doi.org/10.1088/1748-9326/aabf9f, 2018.
  - Gocke, M., Pustovoytov, K., and Kuzyakov, Y.: Carbonate recrystallization in root-free soil and rhizosphere of Triticum aestivum and Lolium perenne estimated by 14C labeling, Biogeochemistry, 103, 209–222, https://doi.org/10.1007/s10533-010-9456-z, 2011.
- 730 Goll, D. S., Ciais, P., Amann, T., Buermann, W., Chang, J., Eker, S., Hartmann, J., Janssens, I., Li, W., Obersteiner, M., Penuelas, J., Tanaka, K., and Vicca, S.: Potential CO2 removal from enhanced weathering by ecosystem responses to powdered rock, Nat. Geosci., 14, 545–549, https://doi.org/10.1038/s41561-021-00798-x, 2021.
  - Goulding, K. W.: Factors affecting soil pH and the use of different liming materials., 2015.
  - Hamilton, S. K., Kurzman, A. L., Arango, C., Jin, L., and Robertson, G. P.: Evidence for carbon sequestration by agricultural
- 735 liming, Glob. Biogeochem. Cycles, 21, 2006GB002738, https://doi.org/10.1029/2006GB002738, 2007.
  - Hartmann, J., West, A. J., Renforth, P., Köhler, P., De La Rocha, C. L., Wolf-Gladrow, D. A., Dürr, H. H., and Scheffran, J.: Enhanced chemical weathering as a geoengineering strategy to reduce atmospheric carbon dioxide, supply nutrients, and mitigate ocean acidification, Rev. Geophys., 51, 113–149, https://doi.org/10.1002/rog.20004, 2013.
  - Hartmann, K.J., Bauriegel, A., Dehner, U., Eberhardt, E., Hesse, S., Kühn, D., Martin, W., Waldmann, F., AG Boden, BGR
- Hannover (Ed.): Bodenkundliche Kartieranleitung KA6 in 2 Bänden, Schweizerbart Science Publishers, Stuttgart, Germany, 2024.
  - Haque, F., Santos, R. M., Dutta, A., Thimmanagari, M., and Chiang, Y. W.: Co-Benefits of Wollastonite Weathering in Agriculture: CO2 Sequestration and Promoted Plant Growth, ACS Omega, 4, 1425–1433, https://doi.org/10.1021/acsomega.8b02477, 2019.
- Heřmanská, M., Voigt, M. J., Marieni, C., Declercq, J., and Oelkers, E.: A comprehensive and consistent mineral dissolution rate database: Part II: Secondary silicate minerals, Chem. Geol., 636, 121632, 2023.
  - Heřmanská, M., Voigt, M. J., Marieni, C., Declercq, J., and Oelkers, E. H.: A comprehensive and internally consistent mineral dissolution rate database: Part I: Primary silicate minerals and glasses, Chem. Geol., 597, 120807, 2022.
  - Holden, F. J., Davies, K., Bird, M. I., Hume, R., Green, H., Beerling, D. J., and Nelson, P. N.: In-field carbon dioxide removal via weathering of crushed basalt applied to acidic tropical agricultural soil, Sci. Total Environ., 955, 176568, https://doi.org/10.1016/j.scitotenv.2024.176568, 2024.
    - Iff, N., Renforth, P., and Pogge von Strandmann, P. A. E.: The dissolution of olivine added to soil at 32°C: the fate of weathering products and its implications for enhanced weathering at different temperatures, Front. Clim., 6, https://doi.org/10.3389/fclim.2024.1252210, 2024.
- 755 IPCC, 2018: Global Warming of 1.5°C. An IPCC Special Report on the impacts of global warming of 1.5°C above preindustrial levels and related global greenhouse gas emission pathways, in the context of strengthening the global response to the threat of climate change, sustainable development, and efforts to eradicate poverty [Masson-Delmotte, V., P. Zhai, H.-O.





- Pörtner, D. Roberts, J. Skea, P.R. Shukla, A. Pirani, W. Moufouma-Okia, C. Péan, R. Pidcock, S. Connors, J.B.R. Matthews, Y. Chen, X. Zhou, M.I. Gomis, E. Lonnoy, T. Maycock, M. Tignor, and T. Waterfield (eds.)]. In Press.
- 760 Kanzaki, Y., Planavsky, N. J., Zhang, S., Jordan, J., Suhrhoff, T. J., and Reinhard, C. T.: Soil cation storage is a key control on the carbon removal dynamics of enhanced weathering, Environ. Res. Lett., 20, 074055, https://doi.org/10.1088/1748-9326/ade0d5, 2025.
  - Kanzaki, Y., Zhang, S., Planavsky, N. J., and Reinhard, C. T.: Soil Cycles of Elements simulator for Predicting TERrestrial regulation of greenhouse gases: SCEPTER v0.9, Geosci. Model Dev., 15, 4959–4990, https://doi.org/10.5194/gmd-15-4959-4959-4950, https://doi.org/10.5194/gmd-15-4959-4950, https://doi.org/10.5194/gmd-15-4950, https://doi.org/10.5194/gmd-15-4950,
- 765 2022, 2022.
  - Kelland, M. E., Wade, P. W., Lewis, A. L., Taylor, L. L., Sarkar, B., Andrews, M. G., Lomas, M. R., Cotton, T. E. A., Kemp, S. J., James, R. H., Pearce, C. R., Hartley, S. E., Hodson, M. E., Leake, J. R., Banwart, S. A., and Beerling, D. J.: Increased yield and CO2 sequestration potential with the C4 cereal Sorghum bicolor cultivated in basaltic rock dust-amended agricultural soil, Glob. Change Biol., 26, 3658–3676, https://doi.org/10.1111/gcb.15089, 2020.
- 770 Leineweber, D.: Production of Calcium Magnesium Acetate (CMA) from Dilute Aqueous Solutions of Acetic Acid, 2002.
  Maher, K.: The dependence of chemical weathering rates on fluid residence time, Earth Planet. Sci. Lett., 294, 101–110, 2010.
  Maher, K. and Chamberlain, C. P.: Hydrologic Regulation of Chemical Weathering and the Geologic Carbon Cycle, Science, 343, 1502–1504, https://doi.org/10.1126/science.1250770, 2014.
  - Maxbauer, D., Milliken, E., Yambing, J. R., Watson, E., Gregg, R. B., Swanson, L., Sohng, J., Sokol, N. W., and Planavsky,
- 775 N.: Evidence for carbon dioxide removal via enhanced rock weathering with steel slag, though not basalt, in a midwestern US field trial, CDRXIV [preprint], cdrxiv.org/preprint/359, 1 July 2025.
  - McDermott, F., Bryson, M., Magee, R., and van Acken, D.: Enhanced weathering for CO2 removal using carbonate-rich crushed returned concrete; a pilot study from SE Ireland, Appl. Geochem., 169, 106056, https://doi.org/10.1016/j.apgeochem.2024.106056, 2024.
- 780 Medicine, N. A. of S., Engineering, and, Studies, D. on E. and L., Board, O. S., Technology, B. on C. S. and, Resources, B. on E. S. and, Resources, B. on E. and E., Climate, B. on A. S. and, and Sequestration, C. on D. a R. A. for C. D. R. and R.: Negative Emissions Technologies and Reliable Sequestration: A Research Agenda, National Academies Press, 511 pp., 2019.
- Middelburg, J. J., Soetaert, K., and Hagens, M.: Ocean Alkalinity, Buffering and Biogeochemical Processes, Rev. Geophys., 58, e2019RG000681, https://doi.org/10.1029/2019RG000681, 2020.
  - Moscatelli, M. C., Massaccesi, L., Marabottini, R., Primavera, F., Riccini, A., and Marinari, S.: The beneficial use of basalt flour combined to a microbial consortium to improve soil quality in basalt and carbonatic dismissed quarries, CATENA, 237, 107820, https://doi.org/10.1016/j.catena.2024.107820, 2024.
- Nye, P. H. and Ameloko, A. Y.: Predicting the rate of dissolution of lime in soil, J. Soil Sci., 38, 641–649, https://doi.org/10.1111/j.1365-2389.1987.tb02161.x, 1987.



810



- Oelkers, E. H., Declercq, J., Saldi, G. D., Gislason, S. R., and Schott, J.: Olivine dissolution rates: A critical review, Chem. Geol., 500, 1–19, https://doi.org/10.1016/j.chemgeo.2018.10.008, 2018.
- Paessler, D., Hammes, J., Smet, I., Steffens, R., Stöckel, A., and Hartmann, J.: Learnings from running the world's largest greenhouse EW experiment, whitepaper, Carbon Drawdown Initiative, https://doi.org/10.13140/RG.2.2.18184.74247, 2025.
- Paessler, D., Steffens, R., and Hammes, J.: Setting up the Carbdown Greenhouse Experiment 2023 (With Recipe And Shopping-list), Blog Our Journey to Negative Emissions, https://www.carbon-drawdown.de/blog/2023-3-16-setting-up-the-carbdown-greenhouse-experiment-2023-with-recipe-and-shopping-list (last access: 20.08.2025), 16.03.2023.
  - Palandri, J. L. and Kharaka, Y. K.: A compilation of rate parameters of water-mineral interaction kinetics for application to geochemical modeling, Open-File Report, U.S. Geological Survey, https://doi.org/10.3133/ofr20041068, 2004.
- te Pas, E. E. M., Chang, E., Marklein, A. R., Comans, R. N. J., and Hagens, M.: Accounting for retarded weathering products in comparing methods for quantifying carbon dioxide removal in a short-term enhanced weathering study, Front. Clim., 6, https://doi.org/10.3389/fclim.2024.1524998, 2025.
  - Pogge von Strandmann, P. A. E., He, X., Zhou, Y., and Wilson, D. J.: Comparing open versus closed system weathering experiments using lithium isotopes, Appl. Geochem., 189, 106458, https://doi.org/10.1016/j.apgeochem.2025.106458, 2025.
- Pogge von Strandmann, P. A. E., Liu, X., Liu, C.-Y., Wilson, D. J., Hammond, S. J., Tarbuck, G., Aristilde, L., Krause, A. J., and Fraser, W. T.: Lithium isotope behaviour during basalt weathering experiments amended with organic acids, Geochim. Cosmochim. Acta, 328, 37–57, https://doi.org/10.1016/j.gca.2022.04.032, 2022a.
  - Pogge von Strandmann, P. A. E., Tooley, C., Mulders, J. J. P. A., and Renforth, P.: The Dissolution of Olivine Added to Soil at 4°C: Implications for Enhanced Weathering in Cold Regions, Front. Clim., 4, https://doi.org/10.3389/fclim.2022.827698, 2022b.
  - Pokrovsky, O. S. and Schott, J.: Kinetics and mechanism of forsterite dissolution at 25°C and pH from 1 to 12, Geochim. Cosmochim. Acta, 64, 3313–3325, https://doi.org/10.1016/S0016-7037(00)00434-8, 2000.
  - Renforth, P., Pogge von Strandmann, P. A. E., and Henderson, G. M.: The dissolution of olivine added to soil: Implications for enhanced weathering, Appl. Geochem., 61, 109–118, https://doi.org/10.1016/j.apgeochem.2015.05.016, 2015.
- Rineau, F., Frank, A. H., Groh, J., Grosjean, K., Legout, A., Kolokolov, D. I., Mench, M., Moreno-Druet, M., Pollier, B., Povilaitis, V., Pausch, J., Puetz, T., Rooks, T., Schröder, P., Szulc, W., Rutkowska, B., Swinnen, X., Thijs, S., Vereecken, H., Veselovskaya, J. V., Zubery, M., Žydelis, R., and Loit, E.: Enhanced weathering leads to substantial C accrual on crop macrocosms, EGUsphere, 1–25, https://doi.org/10.5194/egusphere-2025-4188, 2025.
- Shainberg, I., Levy, G. J., Goldstein, D., Mamedov, A. I., and Letey, J.: Prewetting rate and sodicity effects on the hydraulic conductivity of soils, Soil Res., 39, 1279–1291, 2001.
  - Smith, S. M., Geden, O., Gidden, M. J., Lamb, W. F., Nemet, G. F., Minx, J. C., Buck, H., Burke, J., Cox, E., Edwards, M. R., Fuss, S., Johnstone, I., Müller-Hansen, F., Pongratz, J., Probst, B. S., Roe, S., Schenuit, F., Schulte, I., Vaughan, N. E. (eds.) The State of Carbon Dioxide Removal 2024 2nd Edition. DOI 10.17605/OSF.IO/F85QJ (2024)





- Smith, M. L., Weitz, K. K., Thompson, A. M., Jansson, J. K., Hofmockel, K. S., and Lipton, M. S.: Real-Time and Rapid
- 825 Respiratory Response of the Soil Microbiome to Moisture Shifts, Microorganisms, 11, 2630, https://doi.org/10.3390/microorganisms11112630, 2023.
  - Smith, P.: An overview of the permanence of soil organic carbon stocks: influence of direct human-induced, indirect and natural effects, Eur. J. Soil Sci., 56, 673–680, https://doi.org/10.1111/j.1365-2389.2005.00708.x, 2005.
  - Sparks, D. L., Singh, B., and Siebecker, M. G.: Environmental soil chemistry, Elsevier, 2022.
- 830 Sparks, D. L.: Environmental soil chemistry: An overview, Environ. Soil Chem., 2, 2003.
  Steinwidder, L., Boito, L., Frings, P. J., Niron, H., Rijnders, J., de Schutter, A., Vienne, A., and Vicca, S.: Beyond Inorganic
  C: Soil Organic C as a Key Pathway for Carbon Sequestration in Enhanced Weathering, Glob. Change Biol., 31, e70340, https://doi.org/10.1111/gcb.70340, 2025.
- Taalab, A. S., Ageeb, G. W., Siam, H. S., and Mahmoud, S. A.: Some characteristics of calcareous soils. A review as Taalab1, GW Ageeb2, Hanan S. Siam1 and Safaa A. Mahmoud1, Middle East J, 8, 96–105, 2019.
- Ten Berge, H. F. M., Van Der Meer, H. G., Steenhuizen, J. W., Goedhart, P. W., Knops, P., and Verhagen, J.: Olivine Weathering in Soil, and Its Effects on Growth and Nutrient Uptake in Ryegrass (Lolium perenne L.): A Pot Experiment, PLoS ONE, 7, e42098, https://doi.org/10.1371/journal.pone.0042098, 2012.
- Tessier, A., Campbell, P. G. C., and Bisson, M.: Sequential extraction procedure for the speciation of particulate trace metals, Anal. Chem., 51, 844–851, https://doi.org/10.1021/ac50043a017, 1979.
- Tisdale, S. L., Nelson, W. L., Beaton, J. D., and Havlin, J. L.: Soil Fertility and Fertilizers, Collier Macmillan Publishers, 1985. Vienne, A., Frings, P., Rijnders, J., Suhrhoff, T. J., Reershemius, T., Poetra, R. P., Hartmann, J., Niron, H., Estrada, M. P., Steinwidder, L., Boito, L., and Vicca, S.: Weathering without inorganic CDR revealed through cation tracing, EGUsphere, 2025, 1–24, https://doi.org/10.5194/egusphere-2025-1667, 2025.
- Vienne, A., Poblador, S., Portillo-Estrada, M., Hartmann, J., Ijiehon, S., Wade, P., and Vicca, S.: Enhanced Weathering Using Basalt Rock Powder: Carbon Sequestration, Co-benefits and Risks in a Mesocosm Study With Solanum tuberosum, Front. Clim., 4, https://doi.org/10.3389/fclim.2022.869456, 2022.
  - Vorrath, M.-E., Amann, T., Meyer zu Drewer, J., Hagemann, N., Aldrich, C., Börker, J., Seedtke, M., Becker, J. N., Hagens, M., Eschenbach, A., and Hartmann, J.: Pyrogenic carbon and carbonating minerals for carbon capture and storage (PyMiCCS)
- 850 part II: organic and inorganic carbon dioxide removal in an Oxisol, Front. Clim., 7 https://doi.org/10.3389/fclim.2025.1592454, 2025.
  - Walker, J. C. G., Hays, P. B., and Kasting, J. F.: A negative feedback mechanism for the long-term stabilization of Earth's surface temperature, J. Geophys. Res. Oceans, 86, 9776–9782, https://doi.org/10.1029/JC086iC10p09776, 1981.
  - Wang, J., Keener, T. C., Li, G., and Khang, S.-J.: THE DISSOLUTION RATE OF Ca(OH)2 IN AQUEOUS SOLUTIONS,
- 855 Chemical Engineering Communications, 169, 167–184, https://doi.org/10.1080/00986449808912726, 1998.
  West, A. J., Galy, A., and Bickle, M.: Tectonic and climatic controls on silicate weathering, Earth Planet. Sci. Lett., 235, 211–228, https://doi.org/10.1016/j.epsl.2005.03.020, 2005.

https://doi.org/10.5194/egusphere-2025-5402 Preprint. Discussion started: 24 November 2025 © Author(s) 2025. CC BY 4.0 License.





Wimpenny, J.: Clay Minerals, in: Encyclopedia of Geochemistry, Springer, Cham, 1–11, https://doi.org/10.1007/978-3-319-39193-9 51-1, 2016.

Wolf-Gladrow, D. A., Zeebe, R. E., Klaas, C., Körtzinger, A., and Dickson, A. G.: Total alkalinity: The explicit conservative expression and its application to biogeochemical processes, Mar. Chem., 106, 287–300, https://doi.org/10.1016/j.marchem.2007.01.006, 2007.